
Double Equivariance for Inductive Link Prediction for Both New Nodes and New Relation Types

Anonymous Author(s)

Affiliation

Address

email

Abstract

1 The task of inductive link prediction in discrete attributed multigraphs (e.g., knowl-
2 edge graphs, multilayer networks, heterogeneous networks, etc.) generally focuses
3 on test predictions with solely new nodes but not both new nodes and new relation
4 types. In this work, we formally define the task of predicting (completely) new
5 nodes and new relation types in test as a *doubly inductive link prediction* task
6 and introduce a theoretical framework for the solution. We start by defining the
7 concept of *double permutation-equivariant representations* that are equivariant to
8 permutations of both node identities and edge relation types. We then propose a
9 general blueprint to design neural architectures that impose a structural representa-
10 tion of relations that can inductively generalize from training nodes and relations
11 to arbitrarily new test nodes and relations without the need for adaptation, side
12 information, or retraining. We also introduce the concept of *distributionally double*
13 *equivariant positional embeddings* designed to perform the same task. Finally,
14 we empirically demonstrate the capability of the two proposed models on a set
15 of novel real-world benchmarks, showcasing relative performance gains of up to
16 41.40% on predicting new relations types compared to baselines.

17 1 Introduction

18 This work studies what we call a *doubly inductive* (node and relation) *link prediction*
19 task to predict missing links in unseen discrete attributed multigraphs with completely
20 new nodes and new relation types in test (i.e. none of them are seen in training).
21 Discrete attributed multigraphs encompass knowledge graphs [5, 76, 63, 62, 19, 58],
22 multilayer networks (multiple graph types sharing a common set of nodes, e.g.,
23 the power grid and the road network [16, 17]), and heterogeneous networks
24 with discrete link types (e.g., recommending products to users that have distinct
25 ways to interact with an online store [9, 79, 71]). Our experiments primarily center
26 around knowledge graphs; however, we note that the outlined tasks and methodology
27 can be seamlessly adapted to both multilayer and heterogeneous network data.

28 *The main contribution of our work is a general theoretical framework for **doubly inductive link***
29 ***prediction** on discrete attributed multigraphs and a blueprint to create equivariant neural networks*
30 *for this task (both from structural representations and from positional embeddings).* We will introduce
31 the concept of double equivariant graph models and distributionally equivariant positional graph
32 embedding models, which are equivariant to the overgroup of permutations of nodes and permutations
33 of relations (we review the necessary group theory concepts in Section 2). The majority of today's link
34 prediction works can be broadly divided into a few categories that are either incapable of inductive
35 reasoning over new relations in test or require side information to do so. In Section 4 we explain how
the doubly inductive link prediction is different from these existing tasks in more detail.

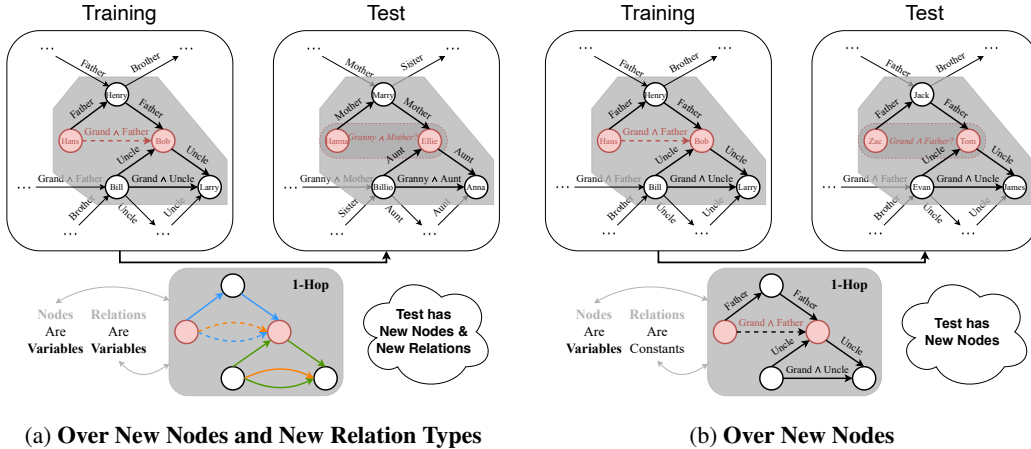


Figure 1: (a) **Doubly inductive link prediction:** In this task, the goal is to learn (on training graphs) to inductively predict querying relation over test graphs with new nodes and new relation types. Sharing local **relational structure** (bottom) enables predicting the same relative relation types w.r.t. the structure of the training pair, as there is a common relational type structure (the colored links) in training that can be applied to the new nodes and new relation in test. (b) **Traditional inductive link prediction:** This task aims to inductively predict querying relation over test graph with only new nodes. Querying node pairs share the same local structure (bottom) as a training pair. Thus, we can predict the same relation type as in training. Since relation types of the local structure are assumed the same in training and test, this approach can only be applied over new nodes.

36 **Contributions.** In this work, we study the task of *doubly inductive link prediction over both new*
 37 *nodes and new relation types, using only information obtained from the training graphs.* Our work
 38 makes the following *three* contributions:

- 39 1. We formally introduce the *doubly inductive link prediction task* and the concept of *double equivari-*
 40 *ance* and *distributionally double equivariant positional embeddings* for graph models, whose node
 41 and pairwise representations are equivariant to the action of the permutation overgroup composed
 42 by the permutation subgroups of node identities, and edge types (relations).
- 43 2. We develop the first general *double equivariant* graph neural network (GNN) framework that is
 44 capable of performing *doubly inductive link prediction*, and introduce an approximately double
 45 equivariant representation built from distributionally double equivariant positional embeddings.
- 46 3. We introduce two real-world benchmark datasets: PediaTypes and WikiTopics, for the newly
 47 proposed doubly inductive link prediction task, and empirically verify inductive link prediction
 48 capabilities of our models over both new nodes and new relation types on these benchmarks.

49 2 Doubly (Node & Relation) Inductive Link Prediction

50 In what follows, we introduce the doubly inductive link prediction task and compare it with the tradi-
 51 tional inductive link prediction task using two examples. We then proceed to theoretically describe
 52 the task in a general setting and propose our double equivariant modeling framework to handle doubly
 53 inductive link prediction task using structural representations and positional embeddings.

54 2.1 Doubly inductive link prediction examples

55 We now introduce doubly inductive link prediction over both new nodes and new relation types
 56 and explain the difference between the traditional inductive link prediction task in Figure 1. The
 57 traditional inductive link prediction task focuses solely on predicting new nodes in the test. To this
 58 end, standard graph neural networks (GNNs) [73, 41] force the neural network to learn structural
 59 node representations [54], which —if used appropriately— allows GNNs to perform *inductive link*
 60 *prediction over new nodes* [30, 60] as shown in Figure 1(b) but does not extrapolate over new
 61 relations.

62 However, the equivariance in GNNs is not enough to perform the doubly inductive link prediction task
 63 in Figure 1(a). Specifically, to be able to *inductively* predict the *Granny \wedge Mother* relation on the test
 64 graph by learning from the *Grand \wedge Father* relation on the training graph, the equivariance property
 65 needs to go beyond just node permutations. To be able to represent the structural properties of the

66 nodes and relations with respect to the structural properties of other nodes and relations, our work
 67 defines an equivariance also in relations. For instance, via double equivariance (we will define the
 68 concept in Section 2.3) it is possible to perform the task of predicting Granny \wedge Mother using the node
 69 and relation structural pattern shown at the bottom of Figure 1(a), which can be formally described
 70 through the logical formula $\forall v_1, v_2, v_3, v_4, v_5 \in \mathcal{V}^{\text{te}}, \forall r_1, r_2, r_3 \in \mathcal{R}^{\text{te}}, (v_1, r_1, v_2) \wedge (v_2, r_1, v_3) \wedge$
 71 $(v_4, r_2, v_3) \wedge (v_3, r_2, v_5) \wedge (v_4, r_2, v_5) \wedge (v_4, r_3, v_5) \implies (v_1, r_1, v_3) \wedge (v_1, r_3, v_3)$, where \mathcal{V}^{te} and
 72 \mathcal{R}^{te} are the (new) vertices and (new) relations observed in test. Additional examples and a more
 73 detailed analysis of the logical statements implied by double equivariance are in Appendices A and B.

74 2.2 Formalizing the doubly inductive link prediction task

75 We now introduce notations and definitions used throughout this paper. First, we formally define
 76 our inductive link prediction task for both new nodes and new relation types, i.e., doubly inductive
 77 link prediction, over discrete attributed multigraph. We denote $[n] := \{1, \dots, n\}$ for any $n \in \mathbb{N}$. Let
 78 $\mathcal{G}^{(\text{tr})} = (\mathcal{V}^{(\text{tr})}, \mathcal{R}^{(\text{tr})}, \mathbf{A}^{(\text{tr})})$ be the training discrete attributed multigraph, where $\mathcal{V}^{(\text{tr})}$ is the set of $N^{(\text{tr})}$
 79 training nodes, $\mathcal{R}^{(\text{tr})}$ is the set of $R^{(\text{tr})}$ training relation types. We also define two associated bijective
 80 mappings $v^{(\text{tr})} : [N^{(\text{tr})}] \rightarrow \mathcal{V}^{(\text{tr})}, r^{(\text{tr})} : [R^{(\text{tr})}] \rightarrow \mathcal{R}^{(\text{tr})}$ that enumerate the nodes and relation types in
 81 training. The tensor $\mathbf{A}^{(\text{tr})} \in \{0, 1\}^{N^{(\text{tr})} \times R^{(\text{tr})} \times N^{(\text{tr})}}$ defines the adjacency of the training graph such that
 82 $\forall (i, k, j) \in [N^{(\text{tr})}] \times [R^{(\text{tr})}] \times [N^{(\text{tr})}], \mathbf{A}_{i,k,j}^{(\text{tr})} = 1$ indicates that the triplet $(v_i^{(\text{tr})}, r_k^{(\text{tr})}, v_j^{(\text{tr})})$ is present
 83 in the data (we denote (i, k, i) as the k -th attribute of node i). To simplify notation, we further refer to
 84 the collection of all discrete attributed multigraph of any sizes as $\mathbb{A} := \cup_{N=1}^{\infty} \cup_{R=2}^{\infty} \{0, 1\}^{N \times R \times N}$.

85 **Definition 2.1** (Doubly inductive link prediction task). The task of doubly inductive link prediction
 86 learns a model on $\mathcal{G}^{(\text{tr})}$ and inductively apply it to predict missing links in a test graph $\mathcal{G}^{(\text{te})} =$
 87 $(\mathcal{V}^{(\text{te})}, \mathcal{R}^{(\text{te})}, \mathbf{A}^{(\text{te})})$ with *completely* new nodes and new relation types, i.e., $\mathcal{V}^{(\text{te})} \cap \mathcal{V}^{(\text{tr})} = \emptyset, \mathcal{R}^{(\text{te})} \cap$
 88 $\mathcal{R}^{(\text{tr})} = \emptyset$, without extra context given to the model. Specifically, we aim to predict both missing
 89 relations for the given head and tail nodes $(i, ?, j)$ and missing nodes for a given relation $(i, k, ?)$.

90 While some real-world tasks may have overlapping relation types between training and test, Defini-
 91 tion 2.1 forces the model to not rely on potential overlaps. In what follows, we use the superscript
 92 $(*)$ as a wildcard to describe both train and test data. For example, $\mathbf{A}^{(*)}$ is a wildcard variable for
 93 referring to either $\mathbf{A}^{(\text{tr})}$ or $\mathbf{A}^{(\text{te})}$. For brevity, we use discrete attributed multigraph and attributed
 94 multigraph interchangeably. And since there are bijections $v^{(*)}, r^{(*)}$ between indices and nodes
 95 and relation types, we represent the triplet $(v_i^{(*)}, r_k^{(*)}, v_j^{(*)}) \in \mathcal{V}^{(*)} \times \mathcal{R}^{(*)} \times \mathcal{V}^{(*)}$ with indices
 96 $(i, k, j) \in [N^{(*)}] \times [R^{(*)}] \times [N^{(*)}]$, and mainly use $\mathbf{A}^{(*)}$ to denote discrete attributed multigraph.

97 Without additional context such as textural description embeddings for the new relations or graph
 98 ontology (thoroughly discussed in Section 4), it is essential for our model to differentiate nodes and
 99 relations based only on their structural relationships in $\mathbf{A}^{(*)}$, rather than their labels in $\mathcal{V}^{(*)}, \mathcal{R}^{(*)}$, in
 100 order to make accurate predictions in doubly inductive link prediction as discussed in Section 2.1.
 101 Thus, we develop the double equivariant representations for attributed multigraphs as follows.

102 2.3 Double equivariant representations for attributed multigraphs

103 In what follows, we provide definitions and theoretical statements of our proposed double equivariant
 104 attributed multigraph representations in the main paper while referring all proofs to Appendix C. The
 105 proposal starts with defining the permutation actions on discrete attributed multigraphs as:

106 **Definition 2.2** (Node and relation permutation actions on attributed multigraphs). For any attributed
 107 multigraph $\mathbf{A}^{(*)} \in \mathbb{A}$ with number of nodes and relations $N^{(*)}, R^{(*)}$, a node permutation $\phi \in \mathbb{S}_{N^{(*)}}$
 108 is an element of the symmetric group $\mathbb{S}_{N^{(*)}}$, a relation permutation $\tau \in \mathbb{S}_{R^{(*)}}$ is an element of the
 109 symmetric group $\mathbb{S}_{R^{(*)}}$, and the operation $\phi \circ \tau \circ \mathbf{A}^{(*)}$ is the action of ϕ and τ on $\mathbf{A}^{(*)}$, defined as
 110 $\forall (i, k, j) \in [N^{(*)}] \times [R^{(*)}] \times [N^{(*)}], (\phi \circ \tau \circ \mathbf{A}^{(*)})_{\phi \circ i, \tau \circ k, \phi \circ j} = \mathbf{A}_{i,k,j}^{(*)}$ where $\phi \circ i = \phi_i$ and $\tau \circ k = \tau_k$.
 111 The node and relation permutation actions on $\mathbf{A}^{(*)}$ are commutative, i.e., $\phi \circ \tau \circ \mathbf{A}^{(*)} = \tau \circ \phi \circ \mathbf{A}^{(*)}$.

112 To learn structural representation for both nodes and relations, we first design triplet representations
 113 that are invariant to the two permutation actions on nodes and relations, as shown below.

114 **Definition 2.3** (Double invariant triplet representations). For any attributed multigraph $\mathbf{A}^{(*)} \in \mathbb{A}$
 115 with number of nodes and relations $N^{(*)}, R^{(*)}$, a double invariant triplet representation is a function
 116 $\Gamma_{\text{tri}} : \cup_{N=1}^{\infty} \cup_{R=2}^{\infty} ([N] \times [R] \times [N]) \times \mathbb{A} \rightarrow \mathbb{R}^d, d \geq 1$, such that $\forall (i, k, j) \in [N^{(*)}] \times [R^{(*)}] \times$
 117 $[N^{(*)}], \forall \phi \in \mathbb{S}_{N^{(*)}}, \forall \tau \in \mathbb{S}_{R^{(*)}}, \Gamma_{\text{tri}}((i, k, j), \mathbf{A}^{(*)}) = \Gamma_{\text{tri}}((\phi \circ i, \tau \circ k, \phi \circ j), \phi \circ \tau \circ \mathbf{A}^{(*)})$.

118 To understand the property of our double invariant triplet representations, we first introduce the notion
 119 of discrete attributed multigraph isomorphism and triplet double isomorphism.

120 **Definition 2.4** (Attributed multigraph isomorphism and Triplet isomorphism). We say two attributed
 121 multigraphs $\mathbf{A}^{(G)}, \mathbf{A}^{(H)} \in \mathbb{A}$ with number of nodes and relations $N^{(G)}, R^{(G)}$ and $N^{(H)}, R^{(H)}$
 122 respectively, are isomorphic (denoted as “ $\mathbf{A}^{(G)} \simeq_{\text{RL}} \mathbf{A}^{(H)}$ ”) if and only if $\exists \phi \in \mathbb{S}_{N^{(G)}}, \exists \tau \in$
 123 $\mathbb{S}_{R^{(G)}}$, such that $\phi \circ \tau \circ \mathbf{A}^{(G)} = \mathbf{A}^{(H)}$. And we say two triplets $(i^{(G)}, k^{(G)}, j^{(G)}) \in [N^{(G)}] \times$
 124 $[R^{(G)}] \times [N^{(G)}], (i^{(H)}, k^{(H)}, j^{(H)}) \in [N^{(H)}] \times [R^{(H)}] \times [N^{(H)}]$ are isomorphic triplets (denoted
 125 as “ $((i^{(G)}, k^{(G)}, j^{(G)}), \mathbf{A}^{(G)}) \simeq_{\text{TRI}} ((i^{(H)}, k^{(H)}, j^{(H)}), \mathbf{A}^{(H)})$ ”) if and only if $\exists \phi \in \mathbb{S}_{N^{(G)}}, \exists \tau \in$
 126 $\mathbb{S}_{R^{(G)}}$, such that $\phi \circ \tau \circ \mathbf{A}^{(G)} = \mathbf{A}^{(H)}$ and $(i^{(H)}, k^{(H)}, j^{(H)}) = (\phi \circ i^{(G)}, \tau \circ k^{(G)}, \phi \circ j^{(G)})$.

127 For example, in Figure 1(a), (Hans, Grand^Father, Bob) in train and (Hanna, Granny^Mother, Ellie)
 128 in test are isomorphic triplets by Definition 2.4 (where “Granny” can be any arbitrary typo in the data).
 129 It is clear that our double invariant triplet representations are able to output the same representations
 130 for these isomorphic triplets, enabling doubly inductive link prediction. The connection between
 131 Definition 2.3 and logical reasoning can be found in Appendix B. In what follows, we define the
 132 structure double equivariant representations for the whole attributed multigraph $\mathbf{A}^{(*)}$ (akin to how
 133 GNNs provide representations for a whole graph).

134 **Definition 2.5** (Double equivariant attributed multigraph representations). For any attributed
 135 multigraph $\mathbf{A}^{(*)} \in \mathbb{A}$ with number of nodes and relations $N^{(*)}, R^{(*)}$, a function $\Gamma_{\text{gra}} : \mathbb{A} \rightarrow$
 136 $\cup_{N=1}^{\infty} \cup_{R=2}^{\infty} \mathbb{R}^{N \times R \times N \times d}, d \geq 1$ is double equivariant w.r.t. arbitrary node $\phi \in \mathbb{S}_{N^{(*)}}$ and relation
 137 $\tau \in \mathbb{S}_{R^{(*)}}$ permutations, if $\Gamma_{\text{gra}}(\phi \circ \tau \circ \mathbf{A}^{(*)}) = \phi \circ \tau \circ \Gamma_{\text{gra}}(\mathbf{A}^{(*)})$. Moreover, valid mappings of
 138 Γ_{gra} must map a domain element to an image element with the same number of nodes and relations.

139 Finally, we connect Definitions 2.3 and 2.5 by showing how to build double equivariant graph
 140 representations from double invariant triplet representations in Theorem 2.6, and vice-versa.

141 **Theorem 2.6.** For all $\mathbf{A}^{(*)} \in \mathbb{A}$ with number of nodes and relations $N^{(*)}, R^{(*)}$, given a double
 142 invariant triplet representation Γ_{tri} , we can construct a double equivariant graph representation as
 143 $(\Gamma_{\text{gra}}(\mathbf{A}^{(*)}))_{i,k,j} := \Gamma_{\text{tri}}((i, k, j), \mathbf{A}^{(*)}), \forall (i, k, j) \in [N^{(*)}] \times [R^{(*)}] \times [N^{(*)}]$, and vice-versa.

144 Next, we consider positional graph embeddings that are equivariant in distribution.

145 2.4 Distributionally double equivariant positional graph embeddings

146 To the best of our knowledge, InGram [35] is the first and only existing work capable of performing
 147 our doubly inductive link prediction task (Definition 2.1), but it does so with what we now define as
 148 *distributionally double equivariant positional embeddings*, which are permutation sensitive, as we
 149 will show in Section 3.2:

150 **Definition 2.7** (Distributionally double equivariant positional embeddings). For any attributed
 151 multigraph $\mathbf{A}^{(*)} \in \mathbb{A}$ with number of nodes and relations $N^{(*)}, R^{(*)}$, the distributionally double
 152 equivariant positional embeddings of $\mathbf{A}^{(*)}$ are defined as joint samples of random variables $\mathbf{Z}|\mathbf{A}^{(*)} \sim$
 153 $p(\mathbf{Z}|\mathbf{A}^{(*)})$, where the tensor \mathbf{Z} is defined as $\mathbf{Z}_{i,k,j} \in \mathbb{R}^d, d \geq 1, \forall (i, k, j) \in [N^{(*)}] \times [R^{(*)}] \times [N^{(*)}]$,
 154 where we say $p(\mathbf{Z}|\mathbf{A}^{(*)})$ is a double equivariant probability distribution on $\mathbf{A}^{(*)}$ defined as $\forall \phi \in$
 155 $\mathbb{S}_{N^{(*)}}, \forall \tau \in \mathbb{S}_{R^{(*)}}, p(\mathbf{Z}|\mathbf{A}^{(*)}) = p(\phi \circ \tau \circ \mathbf{Z}|\phi \circ \tau \circ \mathbf{A}^{(*)})$.

156 Prior work on (standard) link prediction tasks has shown the advantages of equivariant representations
 157 over positional embeddings [84]. Moreover, Srinivasan & Ribeiro (2020) [54] establishes the
 158 equivalence between positional embeddings and structural representations for simple graphs by
 159 proving that representations based on an expectation of the positional embeddings are equivariant to
 160 node permutations. In what follows, we extend this result to the double equivariant setting:

161 **Theorem 2.8** (From distributional double equivariant positional embeddings to double equivariant
 162 representations). For any attributed multigraph $\mathbf{A}^{(*)} \in \mathbb{A}$, the average $\mathbb{E}_{p(\mathbf{Z}|\mathbf{A}^{(*)})}[\mathbf{Z}|\mathbf{A}^{(*)}]$ is a
 163 double equivariant attributed multigraph representation (Definition 2.5) for any distributional double
 164 equivariant positional embeddings $\mathbf{Z}|\mathbf{A}^{(*)}$ (Definition 2.7).

165 Later in Section 3.2, we use the result in Theorem 2.8 to introduce DEq-InGram, a double equivariant
 166 representation that builds upon InGram’s distributionally double equivariant positional embeddings
 167 (Definition 2.7) that is shown to significantly outperforms the original InGram in Section 5.

168 3 Double Equivariant Neural Architecture

169 This section introduces two double equivariant neural architectures based on Sections 2.3 and 2.4.
 170 First, Section 3.1 introduces an Inductive Structural Double Equivariant Architecture (ISDEA), a
 171 model guaranteed to produce double equivariant representations (Definition 2.5). Then, Section 3.2
 172 introduces a Monte Carlo estimate of a double equivariant representation built from a distributionally
 173 double equivariant positional graph embedding [35].

174 3.1 Inductive Structural Double Equivariant Architecture (ISDEA)

175 We start revisiting Definition 2.4. Consider an arbitrary discrete attributed multigraph
 176 $\mathbf{A}^{(*)} \in \mathbb{A}$ with number of nodes and relations
 177 $N^{(*)}, R^{(*)}$, and denote $A^{(*,k)}$ as the adjacency
 178 matrix such that $A_{i,j}^{(*,k)} := \mathbf{A}_{i,k,j}^{(*)}, \forall (i, k, j) \in$
 179 $[N^{(*)}] \times [R^{(*)}] \times [N^{(*)}]$. For each adjacency
 180 matrix $A^{(*,k)}$, it will correspond to a graph with-
 181 out edge relation types, thus we can also consid-
 182 er $A^{(*,k)}$ as an unattributed graph containing
 183 only edges with relation type $r_k^{(*)}$. Then, the
 184 attributed multigraph $\mathbf{A}^{(*)}$ can be equivalently
 185 expressed as a collection of unattributed graphs
 186 $A^{(*)} := \{ \{ A^{(*,1)}, \dots, A^{(*,R^{(*)})} \} \}$. Since the
 187 actions of the two permutation groups $\mathbb{S}_{N^{(*)}}$ and
 188 $\mathbb{S}_{R^{(*)}}$ commute, the double equivariance of $\mathbf{A}^{(*)}$
 189 (Definition 2.4) can be described as two (single)
 190 equivariences: A (graph) equivariance $\phi \in$
 191 $\mathbb{S}_{N^{(*)}}$ over each graph $A^{(*,k)}, k = 1, \dots, R^{(*)}$,
 192 and a (set) equivariance $\tau \in \mathbb{S}_{R^{(*)}}$ (over the set
 193 of graphs). Hence, our double equivariance can
 194 make use of the general framework using DSS
 195 layers on learning sets of symmetric elements
 196 proposed by Maron et al. (2020) [39]. We first
 197 define a double equivariant layer composed by
 198 a Siamese layer [7] as follows, $L : \mathbb{A} \rightarrow \cup_{N=1}^{\infty} \cup_{R=2}^{\infty} \mathbb{R}^{N \times R \times N \times d}$, for each $k = 1, \dots, R^{(*)}$:

$$(L(\mathbf{A}^{(*)}))_{:,k} = L_1(A^{(*,k)}) + L_2(\text{AGG}_{k' \neq k}^{R^{(*)}}(A^{(*,k')})), \quad (1)$$

200 where d is the output dimension, $L_1, L_2 : \mathbb{A} \rightarrow \cup_{N=1}^{\infty} \mathbb{R}^{N \times N \times d}$ can be any (node) equivariant layers
 201 that output pairwise representations [83, 87, 84], and the aggregation term $\text{AGG}_{k' \neq k}^{R^{(*)}}$ can be any set
 202 aggregators such as sum, mean, max, DeepSets [80], etc.. Note that the proposed layer is similar to
 203 the H -equivariant layer proposed by Bevilacqua et al. (2021) [4] for increasing the expressiveness of
 204 GNN using sets of subgraphs (a markedly different task than ours). An illustration of Equation (1) is
 205 provided in Figure 2. We create our double equivariant neural network by stacking double equivariant
 206 layers.

207 3.1.1 Implementation Details

208 We use GNN layers for constructing L_1, L_2 . Since most-expressive pairwise representations are com-
 209 putationally expensive, we propose Inductive Structural Double Equivariant Architecture (ISDEA)
 210 and trade-off expressivity in the implementation of Equation (1) for speed and memory by using node
 211 representation GNN layers [73, 65, 41]. Specifically, for an attributed multigraph $\mathbf{A}^{(*)}$ with number
 212 of nodes and relations $N^{(*)}, R^{(*)}$, at each iteration $t = 1, \dots, T$, all nodes $i \in [N^{(*)}]$ are associated
 213 with a learned vector $h_i^{(t)} \in \mathbb{R}^{R^{(*)} \times d_t}, d_t \geq 1$. If there are no node attributes, we initialize $h_i^{(0)} = \mathbb{1}$
 214 and $d_0 = 1$. Then we recursively compute the update, $\forall i \in [N^{(*)}], \forall k \in [R^{(*)}]$,

$$h_{i,k}^{(t+1)} = \text{GNN}_1^{(t)}\left(h_{i,k}^{(t)}, \left\{ \left\{ h_{j,k}^{(t)} \mid j \in \mathcal{N}_k(i) \right\} \right\}\right) + \text{GNN}_2^{(t)}\left(\text{AGG}_{k' \neq k}^{R^{(*)}}\left(h_{i,k'}^{(t)}\right), \left\{ \left\{ \text{AGG}_{k' \neq k}^{R^{(*)}}\left(h_{j,k'}^{(t)}\right) \mid j \in \bigcup_{k' \neq k} \mathcal{N}_{k'}(i) \right\} \right\}\right),$$

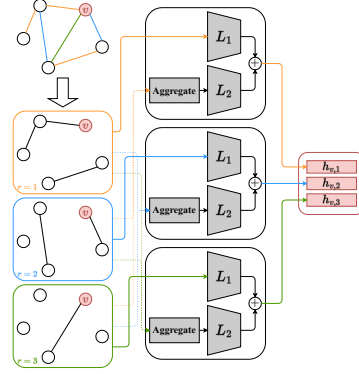


Figure 2: **Illustration of Equation (1):** Attributed multigraph input is split into a set of unattributed graphs $A^{(*,k)}$ corresponding to each relation $k = 1, \dots, R^{(*)}$. For each relation k , the representation of $A^{(*,k)}$ and the set representation of all other unattributed graphs are combined together to update representation $h_{i,k}$ for arbitrary node i . Finally, updated representations of all relations are concatenated together to generate the output h_i .

215 where $\text{GNN}_1^{(t)}$ and $\text{GNN}_2^{(t)}$ denote two GNN layers and $\mathcal{N}_k(i) := \{j \mid \mathbf{A}_{j,k,i}^{(*)} = 1\}$ denotes the
 216 neighborhood set of node i with relation k in the unattributed graph $\mathbf{A}^{(*,k)}$. At the final layers, we
 217 use standard MLPs instead of GNNs to output a final prediction. We use *mean* as our aggregators.

218 As shown by Srinivasan & Ribeiro (2020) [54] and You et al. (2019) [78], structural node representa-
 219 tions are not most expressive for link prediction in unattributed graphs. Hence, we concatenate i and
 220 j (double equivariant) node representations with the shortest distance between i and j in the observed
 221 graph as our triplet representations (appending distances is also adopted in the representations of
 222 prior work [60, 22]). Finally, we obtain the triplet representation,

$$\Gamma_{\text{ISDEA}}((i, k, j), \mathbf{A}^{(*)}) = \left(h_{i,k}^{(T)} \parallel h_{j,k}^{(T)} \parallel d(i, j) \parallel d(j, i) \right), \forall (i, k, j) \in [N^{(*)}] \times [R^{(*)}] \times [N^{(*)}], \quad (2)$$

223 where we denote $d(i, j)$ as the length of shortest path from i to j without considering (i, k, j) , \parallel as
 224 the concatenation operation. Since our graph is directed, we concatenate them in both directions.

225 **Lemma 3.1.** Γ_{ISDEA} in Equation (2) is a double invariant triplet representation as per Definition 2.3.

226 As in Yang et al. (2015) [76]; Schlichtkrull et al. (2018) [53]; Zhu et al. (2021) [87], we use
 227 negative sampling in our training with the difference that we account for both predicting missing
 228 nodes and relation types (Definition 2.1). Specifically, for each positive training triplet (i, k, j)
 229 such that $\mathbf{A}_{i,k,j}^{(\text{tr})} = 1$, we first randomly corrupt either the head or the tail n_{nd} times to generate
 230 the negative (node) examples (i, k, j') . Additionally, we also want our model to learn the correct
 231 relation type $(i, ?, j)$ between a pair of nodes. Thus, we corrupt relation n_{rl} times to generate negative
 232 (relation) examples (i, k', j) . In our training, $n_{\text{nd}} = n_{\text{rl}} = 2$; while in evaluation, $n_{\text{nd}} = 50, n_{\text{rl}} = 0$
 233 for node evaluation, and $n_{\text{nd}} = 0, n_{\text{rl}} = 50$ for relation evaluation. Following Schlichtkrull et al.
 234 (2018) [53], we use cross-entropy loss to encourage the model to score positive examples higher than
 235 corresponding negative examples:

$$\mathcal{L} = - \sum_{(i,k,j) \in \mathcal{S}} \left(\log \left(\Gamma_{\text{tri}}((i, k, j), \mathbf{A}^{(\text{tr})}) \right) - \frac{1}{n_{\text{nd}} + n_{\text{rl}}} \sum_{p=1}^{n_{\text{nd}} + n_{\text{rl}}} \log \left(1 - \Gamma_{\text{tri}} \left((i'_p, k'_p, j'_p), \mathbf{A}^{(\text{tr})} \right) \right) \right), \quad (3)$$

236 where $\mathcal{S} = \{(i, k, j) \mid \mathbf{A}_{i,k,j}^{(\text{tr})} = 1\}$, and (i'_p, k'_p, j'_p) are the p -th negative node or relation example
 237 corresponding to (i, k, j) .

238 3.2 Double Equivariant InGram (DEq-InGram)

239 ISDEA directly obtains double equivariant representations for attributed multigraphs. Alternatively,
 240 one can build these double equivariant representations from distributionally double equivariant
 241 positional embeddings (Theorem 2.8). To this end, we investigate obtaining double equivariant
 242 representations from the positional embeddings of InGram [35], as discussed in Section 2.4.

243 InGram [35] constructs a *relation graph* as a weighted graph consisting of relations and a heuristic to
 244 construct affinity weights between them. It then employs a GNN on the relation graph to generate
 245 relation embeddings, which are then fed into another GNN on the original attributed multigraph to
 246 generate node embeddings. Finally, InGram uses a variant of DistMult [76] to compute triplet scores
 247 from the node and relation embeddings. These embeddings, however, are permutation sensitive due
 248 to their reliances on Glorot initialization [28] in each training epoch and test-time inference.

249 **Lemma 3.2.** *The triplet representations generated by InGram [35] output distributionally double*
 250 *equivariant positional embeddings (Definition 2.7).*

251 Theorem 2.8 suggests that averaging InGram’s positional embeddings can be used to construct double
 252 equivariant attributed multigraph representations. Hence, we propose a Monte Carlo method to
 253 estimate these double equivariant graph representations and denote it as DEq-InGram. Specifically,
 254 given InGram’s triplet score function $\mathbf{Z}_{\text{InGram}}((i, k, j), \mathbf{A}^{(\text{te})}, \mathbf{V}^{(0)}, \mathbf{R}^{(0)})$ over a test attributed multi-
 255 graph $\mathbf{A}^{(\text{te})}$, the initial random node embeddings $\mathbf{V}^{(0)} \in \mathbb{R}^{N^{(\text{te})} \times d}$, and the initial random relation
 256 embeddings $\mathbf{R}^{(0)} \in \mathbb{R}^{R^{(\text{te})} \times d'}$ (where d and d' are the dimension sizes), our DEq-InGram produces
 257 the following triplet scores:

$$\Gamma_{\text{DEq-InGram}}((i, k, j), \mathbf{A}^{(\text{te})}) = \frac{1}{M} \sum_{m=1}^M \mathbf{Z}_{\text{InGram}}((i, k, j), \mathbf{A}^{(\text{te})}, \mathbf{V}_m^{(0)}, \mathbf{R}_m^{(0)}) \quad (4)$$

258 where $\{\mathbf{V}_m^{(0)}\}_{m=1}^M$ and $\{\mathbf{R}_m^{(0)}\}_{m=1}^M$ are M i.i.d. samples drawn from the distribution of initial node
259 and initial relation embeddings respectively (via Glorot initialization).

260 4 Related Work

261 A more comprehensive discussion of related work can be found in Appendix D.

262 **Transductive link prediction.** In transductive link prediction task, missing links are predicted over
263 a fixed set of nodes and relation types as in training [5, 76, 63]. These (positional) embeddings can
264 be made inductive via Srinivasan & Ribeiro (2020) [54]’s theory but are not designed for predicting
265 new relation types.

266 **Inductive link prediction over new nodes (but not new relations).** Rule-induction methods [76,
267 77, 40, 51] are inherently node-independent which aim to extract First-order Logical Horn clauses
268 from the attributed multigraph. Recently, with the advancement of GNNs, various works [53, 60,
269 22, 87, 14] have applied the idea of GNN in relational prediction to learn structural node/pairwise
270 representation. Although all these methods can be used to perform *inductive link prediction over*
271 *solely new nodes*, they can not handle new relation types in test.

272 **Inductive link prediction over both new nodes and new relations (with extra context).** Existing
273 methods for querying triplets involving both new nodes and new relations generally assume access
274 to extra context, such as generating language embedding for textual descriptions of unseen relation
275 types [46, 24, 81, 67], a shared background graph connecting seen and unseen relations (e.g., test
276 graph has training relations [31, 10, 12]), or access to graph ontology [25]. Hence, these methods
277 cannot be directly applied to test graphs that neither contain meaningful descriptive information of the
278 unseen relation types (e.g., url links) nor connection with nodes and relation types seen in training.

279 **Inductive link prediction over both new nodes and new relations (no extra context).** We focus
280 on this most general doubly inductive link prediction task without additional context data (just the
281 test graph structure is available during inference). To the best of our knowledge, InGram [35] is the
282 first and only existing method capable of performing this task. The connection between InGram and
283 our work has been described in Sections 2.4 and 3.2.

284 5 Experimental Results

285 In this section, we aim to answer two questions: **Q1:** Can double equivariant models (ISDEA and
286 DEq-InGram) perform doubly inductive link prediction over attributed multigraphs more accurately
287 than existing methods? **Q2:** Will ISDEA be more stable than DEq-InGram, and will DEq-InGram in
288 turn be more stable than the original InGram [35]? It’s essential to remember that, as per our theory
289 in Section 2, ISDEA is designed to directly produce double equivariant representations. In contrast,
290 InGram yields positional embeddings that achieve double equivariance only in expectation.

291 **Datasets.** To the best of our knowledge, there are no existing real-world benchmarks that are specially
292 designed to test a model’s extrapolation capability for doubly inductive link prediction task with
293 training and test graphs coming from distinct domains with distinct characteristics. Existing datasets
294 such as NL-100, WK-100, and FB-100 from Lee et al. (2023) [35] are typically created by randomly
295 splitting a larger graph (e.g., NELL-995 [72], Wikidata68K [26], FB15K237 [61]) into disjoint node
296 and relation sets, implying that the test and training graphs still come from the same distribution. In
297 contrast, we purposefully create two doubly inductive link prediction benchmark datasets: PediaTypes
298 and WikiTopics, sampled respectively from the OpenEA library [57] and WikiData-5M [68], where
299 by design, the test and training graphs are either from different domains or different topic groups, and
300 are likely to possess different characteristics to fully test model’s capability for doubly inductive link
301 prediction.

302 **Baselines.** To the best of our knowledge, InGram [35] is the first and only work capable of performing
303 doubly inductive link prediction without needing significant modification to the model. We also run
304 RMPi [25], which is capable of reasoning over new nodes and new relations but requires extra context
305 at test time (test graphs either contain training relations or ontology about unseen relations). In
306 addition, we consider the state-of-the-art link prediction model NBFNet [87] capable of generalizing
307 to new nodes but not new relations and modify its architecture to work with new relations at test time

Table 1: **Relation & Node Hits@10 performance on Doubly Inductive Link Prediction over PediaTypes.** We report standard deviations over 5 runs. A higher value means better doubly inductive link prediction performance. The dataset name “ X - Y ” means training on graph X and testing on graph Y . The best values are shown in bold font, while the second-best values are underlined. The highest standard deviation within each task is highlighted in red color. “Rand” column contains unbiased estimations of the performance from a random predictor. **Both ISDEA and DEq-InGram consistently achieve better results than the baselines with generally smaller standard deviations.** N/A*: Not available due to constant crashes.

(a) Relation prediction ($i, ?, j$) performance in %. Higher \uparrow is better.

Models	EN-FR	FR-EN	EN-DE	DE-EN	DB-WD	WD-DB	DB-YG	YG-DB
Rand	19.60±00.00	19.60±00.00	19.60±00.00	19.60±00.00	19.60±00.00	19.60±00.00	19.60±00.00	19.60±00.00
GAT	18.58±00.52	18.93±00.33	19.40±00.28	18.87±00.19	18.78±00.28	18.76±00.33	19.78±01.39	19.15±00.35
GIN	19.34±00.32	19.34±00.29	18.98±00.27	18.88±00.47	19.30±00.52	18.86±00.35	18.69±00.75	18.92±00.68
GraphConv	19.18±00.27	19.02±00.64	19.19±00.24	18.93±00.60	19.46±00.38	19.13±00.54	19.13±01.24	18.89±00.57
NBFNet	21.93±02.53	22.20±02.92	18.98±02.75	7.01±01.43	23.51±07.06	23.05±03.55	31.50±04.82	35.17±05.13
RMPI	27.91±06.48	28.62±03.75	27.51±06.48	25.59±06.48	N/A*	16.76±04.03	39.03±20.28	11.77±07.07
InGram	78.74±07.48	62.11±13.60	48.72±08.94	65.60±14.42	77.75±06.60	63.32±02.78	67.98±25.45	64.98±26.69
DEq-InGram (Ours)	87.94±05.68	80.47±09.90	68.89±05.45	80.79±10.51	91.47±01.53	77.03±04.09	77.72±21.92	89.30±05.53
ISDEA (Ours)	84.94±05.00	84.75±02.51	95.26±00.63	94.23±00.71	82.22±02.44	88.87±02.94	91.42±01.79	85.34±01.49

(b) Node prediction ($i, k, ?$) performance in %. Higher \uparrow is better.

Models	EN-FR	FR-EN	EN-DE	DE-EN	DB-WD	WD-DB	DB-YG	YG-DB
Rand	19.60±00.00	19.60±00.00	19.60±00.00	19.60±00.00	19.60±00.00	19.60±00.00	19.60±00.00	19.60±00.00
GAT	89.77±00.41	86.83±00.41	66.24±02.81	69.08±00.66	31.08±01.07	77.05±00.36	53.51±00.29	64.13±00.31
GIN	90.10±00.61	85.32±01.18	73.32±03.35	75.66±04.85	34.87±09.12	78.67±02.46	56.87±00.44	65.27±01.14
GraphConv	92.97±00.11	90.56±00.04	83.58±00.68	82.64±00.65	40.59±01.72	79.28±01.29	68.91±00.51	76.50±00.14
NBFNet	87.64±01.81	89.77±00.80	85.56±02.07	59.78±03.73	63.23±03.65	78.24±00.90	49.97±01.44	66.36±02.64
RMPI	89.59±06.61	81.79±02.17	82.93±03.56	81.38±06.19	N/A*	65.76±07.45	55.67±06.61	71.03±02.12
InGram	92.32±01.00	83.71±03.53	90.82±01.84	92.15±00.90	61.44±09.84	87.60±01.21	54.79±08.81	67.84±06.38
DEq-InGram (Ours)	94.47±00.60	88.90±02.06	93.85±00.36	94.02±00.74	71.94±07.37	91.47±00.62	71.53±04.78	80.53±07.96
ISDEA (Ours)	76.28±00.05	77.51±01.46	82.24±00.94	81.80±00.68	66.69±01.01	75.19±03.12	72.87±01.03	76.41±01.52

308 (following Lee et al. (2023) [35]’s approach). We also compare our models with message-passing
309 GNNs, including GAT [64], GIN [73], GraphConv [41], which treats the graph as a homogeneous
310 graph by ignoring the relation types. For fair comparisons, we add distance features as in Equation (2)
311 to increase the expressiveness of these GNNs. Additional baseline details are in Appendix E.

312 **Relation and Node Prediction Tasks.** We report the Hits@10 performances over 5 runs of different
313 random seeds for all models on both the relation prediction task of ($i, ?, j$) and the more traditional
314 node prediction task of ($i, k, ?$). For each task, we sample 50 negative triplets for each ground-truth
315 positive target triplet during test evaluation by corrupting the relation type or the tail node respectively.
316 *Further experiment details on synthetic tasks, additional datasets from Lee et al. (2023) [35], baseline*
317 *implementations, ablation studies, and other metrics (e.g., MRR, Hits@1) can be found in Appendix E.*

318 5.1 Doubly Inductive Link Prediction over PediaTypes Dataset

319 The OpenEA library [57] contains multiple attributed multigraphs of relational databases (i.e.,
320 knowledge graphs) from different domains on similar topics, such as DBPedia [36] in different
321 languages (English, French and German), YAGO [48] and Wikidata [66]. We create a new dataset
322 **PediaTypes** (details in Appendix E.1.2) by sampling from the OpenEA library [57], including pairs of
323 attributed multigraphs such as English-to-French DBPedia (denoted as EN-FR), DBPedia-to-YAGO
324 (denoted as DB-YG), etc.. In each graph, triplets are randomly divided into 80% training, 10%
325 validation, and 10% test. We then train and validate the model on one of the graphs (e.g., EN) and
326 directly apply it to another graph (e.g., DE), which has completely new nodes and new relation types.

327 Table 1a shows the results on the relation prediction task, and Table 1b shows the node prediction
328 task on PediaTypes. Across all scenarios on both tasks, our models, ISDEA and DEq-InGram, obtain
329 significantly better average performance, achieving up to 41.40% relative improvement in relation
330 prediction and up to 13.78% relative improvement in node prediction compared to the best-performing
331 baseline. Furthermore, ISDEA tends to have smaller standard deviations than DEq-InGram, and both
332 demonstrate much smaller standard deviations than InGram in almost all scenarios, corroborating our
333 theoretical predictions in Section 2 that a model directly producing double equivariant representations
334 will be more stable than positional embeddings, which are only double equivariant in expectation.

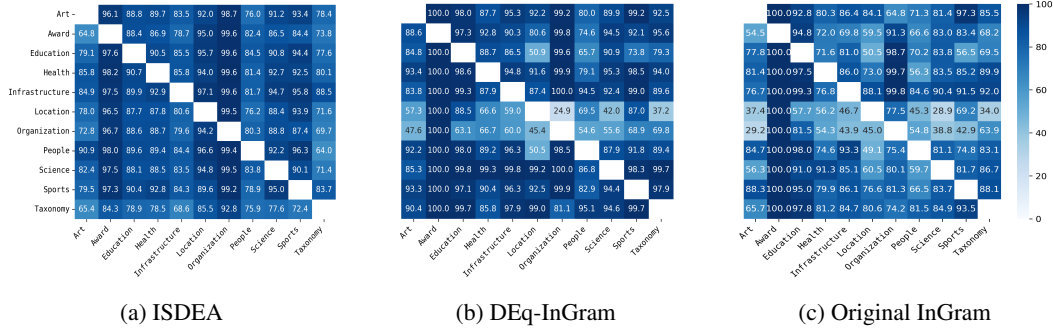


Figure 3: **Relation Hits@10 performance over WikiTopics** for ISDEA, DEq-InGram, and InGram [35]. Each row corresponds to a training graph, and each column corresponds to a test graph. A darker color means better performance. **Both ISDEA and DEq-InGram consistently show better performance than the baseline InGram. In addition, ISDEA exhibits more consistent results across different train-test scenarios than DEq-InGram.**

335 Interestingly, we observe that in the node prediction task, the message-passing GNNs (GAT, GIN,
 336 and GraphConv) achieve quite excellent performances, even though *they completely disregard the*
 337 *information carried by different relation types and treat the attributed multigraph as a homogeneous*
 338 *graph*. This observation corroborates with the conclusions of Jambor et al. (2021) [32]. Indeed, only
 339 4 out of 8 scenarios did InGram outperform the message-passing GNNs on this task, suggesting the
 340 node prediction task might be too easy because a homogeneous link prediction model can do decently
 341 well.

342 5.2 Doubly Inductive Link Prediction over WikiTopics Dataset

343 WikiData-5M [68] is a large knowledge graph dataset containing over 4M entities, 20M triplets,
 344 and 822 relation types from the Wikipedia website. The vast number of relation types span a wide
 345 range of topics, such as arts and media, education and academics, sports and gaming, etc.. Hence, an
 346 interesting question arises: can a model learn on the subgraph corresponding to only one topic, e.g.,
 347 arts, and be directly applicable to reasoning on the subgraph of another topic, e.g., education? To
 348 this end, we create another new dataset **WikiTopics** containing a collection of 11 different attributed
 349 multigraphs, each containing relation types specific to only a particular topic. These graphs are
 350 created by first breaking all relation types of WikiData-5M [68] into 11 non-overlapping topic groups
 351 and then selecting triplets within each topic group (details and statistics in Appendix E.1.3). We train
 352 the models on each of the 11 graphs for 5 random seeds, and for each trained model checkpoint, we
 353 cross-test it on all the other 10 graphs, resulting in a total of 550 statistics. We report the mean results
 354 across random seeds in heatmaps.

355 Figure 3 shows the results of ISDEA, DEq-InGram, and InGram on WikiTopics for the relation
 356 prediction task. The results on the relatively easier task of node prediction are relegated to Ap-
 357 pendix E.1.3. In general, we observe that both ISDEA and DEq-InGram showcase darker colors than
 358 the baseline InGram on the heatmaps, indicating more accurate predictions. In addition, the results
 359 of ISDEA are more consistent than DEq-InGram across different train-test scenarios. For example,
 360 whereas the worst performance of DEq-InGram is 24.9% Hits@10 on LOCATION-ORGANIZATION,
 361 ISDEA’s worst performance is 64.0% Hits@10 on PEOPLE-TAXONOMY. This further corroborates
 362 that a model directly modeling double equivariant representations will be more stable than positional
 363 methods, not only across different random seeds, *but also across different training and test scenarios.*

364 6 Conclusion

365 This work formally introduced the doubly inductive link prediction task defined over both new nodes
 366 and new relation types in the test data. It also defined *double equivariant models* and *distributionally*
 367 *double equivariant positional embedding* models for this task. We showed that, similar to how node
 368 equivariants impose learning structural node representations in unattributed graphs, double (node
 369 and relation) equivariants impose relational structure learning for attributed multigraphs. We then
 370 introduced a blueprint for double equivariant neural network architectures that enables inductive link
 371 prediction over new nodes and relations without the need for additional data or test-time adaptations.
 372 Finally, we proposed two real-world doubly inductive link prediction benchmarks, and empirically
 373 verified the ability of our proposed approaches to extrapolate to both new nodes and relation types.

374 **References**

- 375 [1] Ralph Abboud, Ismail Ilkan Ceylan, Martin Grohe, and Thomas Lukasiewicz. The sur-
 376 prising power of graph neural networks with random node initialization. *arXiv preprint*
 377 *arXiv:2010.01179*, 2020.
- 378 [2] Pablo Barcelo, Mikhail Galkin, Christopher Morris, and Miguel Romero Orth. Weisfeiler and
 379 leman go relational. *arXiv preprint arXiv:2211.17113*, 2022.
- 380 [3] Pablo Barceló, Egor Kostylev, Mikael Monet, Jorge Pérez, Juan Reutter, and Juan-Pablo Silva.
 381 The logical expressiveness of graph neural networks. In *8th International Conference on*
 382 *Learning Representations (ICLR 2020)*, 2020.
- 383 [4] Beatrice Bevilacqua, Fabrizio Frasca, Derek Lim, Balasubramaniam Srinivasan, Chen Cai,
 384 Gopinath Balamurugan, Michael M Bronstein, and Haggai Maron. Equivariant subgraph
 385 aggregation networks. In *International Conference on Learning Representations*, 2021.
- 386 [5] Antoine Bordes, Nicolas Usunier, Alberto Garcia-Duran, Jason Weston, and Oksana Yakhnenko.
 387 Translating embeddings for modeling multi-relational data. *Advances in neural information*
 388 *processing systems*, 26, 2013.
- 389 [6] Shaked Brody, Uri Alon, and Eran Yahav. How attentive are graph attention networks? *arXiv*
 390 *preprint arXiv:2105.14491*, 2021.
- 391 [7] Jane Bromley, Isabelle Guyon, Yann LeCun, Eduard Säckinger, and Roopak Shah. Signature
 392 verification using a " siamese" time delay neural network. *Advances in neural information*
 393 *processing systems*, 6, 1993.
- 394 [8] Michael M Bronstein, Joan Bruna, Yann LeCun, Arthur Szlam, and Pierre Vandergheynst.
 395 Geometric deep learning: going beyond euclidean data. *IEEE Signal Processing Magazine*,
 396 34(4):18–42, 2017.
- 397 [9] Chong Chen, Weizhi Ma, Min Zhang, Zhaowei Wang, Xiuqiang He, Chenyang Wang, Yiqun
 398 Liu, and Shaoping Ma. Graph heterogeneous multi-relational recommendation. In *Proceedings*
 399 *of the AAAI Conference on Artificial Intelligence*, volume 35, pages 3958–3966, 2021.
- 400 [10] Jiajun Chen, Huarui He, Feng Wu, and Jie Wang. Topology-aware correlations between relations
 401 for inductive link prediction in knowledge graphs. In *Proceedings of the AAAI Conference on*
 402 *Artificial Intelligence*, volume 35, pages 6271–6278, 2021.
- 403 [11] Mingyang Chen, Wen Zhang, Yuxia Geng, Zezhong Xu, Jeff Z Pan, and Huajun Chen. General-
 404 izing to unseen elements: A survey on knowledge extrapolation for knowledge graphs. *arXiv*
 405 *preprint arXiv:2302.01859*, 2023.
- 406 [12] Mingyang Chen, Wen Zhang, Zhen Yao, Xiangnan Chen, Mengxiao Ding, Fei Huang, and
 407 Huajun Chen. Meta-learning based knowledge extrapolation for knowledge graphs in the
 408 federated setting. In Lud De Raedt, editor, *Proceedings of the Thirty-First International*
 409 *Joint Conference on Artificial Intelligence, IJCAI-22*, pages 1966–1972. International Joint
 410 Conferences on Artificial Intelligence Organization, 7 2022. Main Track.
- 411 [13] Mingyang Chen, Wen Zhang, Wei Zhang, Qiang Chen, and Huajun Chen. Meta relational learn-
 412 ing for few-shot link prediction in knowledge graphs. In *Proceedings of the 2019 Conference on*
 413 *Empirical Methods in Natural Language Processing and the 9th International Joint Conference*
 414 *on Natural Language Processing (EMNLP-IJCNLP)*, pages 4217–4226, 2019.
- 415 [14] Yihong Chen, Pushkar Mishra, Luca Franceschi, Pasquale Minervini, Pontus Stenetorp, and
 416 Sebastian Riedel. Refactor gnns: Revisiting factorisation-based models from a message-passing
 417 perspective. In *Advances in Neural Information Processing Systems*, 2022.
- 418 [15] Kewei Cheng, Jiahao Liu, Wei Wang, and Yizhou Sun. Rlogic: Recursive logical rule learning
 419 from knowledge graphs. In *Proceedings of the 28th ACM SIGKDD Conference on Knowledge*
 420 *Discovery and Data Mining*, pages 179–189, 2022.
- 421 [16] Michele Coscia, Giulio Rossetti, Diego Pennacchioli, Damiano Ceccarelli, and Fosca Giannotti.
 422 " you know because i know" a multidimensional network approach to human resources prob-
 423 lem. In *Proceedings of the 2013 IEEE/ACM International Conference on Advances in Social*
 424 *Networks Analysis and Mining*, pages 434–441, 2013.
- 425 [17] Manlio De Domenico, Albert Solé-Ribalta, Emanuele Cozzo, Mikko Kivelä, Yamir Moreno,
 426 Mason A Porter, Sergio Gómez, and Alex Arenas. Mathematical formulation of multilayer
 427 networks. *Physical Review X*, 3(4):041022, 2013.

- 428 [18] Michaël Defferrard, Xavier Bresson, and Pierre Vandergheynst. Convolutional neural networks
429 on graphs with fast localized spectral filtering. *Advances in neural information processing*
430 *systems*, 29, 2016.
- 431 [19] Tim Dettmers, Pasquale Minervini, Pontus Stenetorp, and Sebastian Riedel. Convolutional 2d
432 knowledge graph embeddings. In *Proceedings of the AAAI conference on artificial intelligence*,
433 volume 32, 2018.
- 434 [20] Chelsea Finn, Pieter Abbeel, and Sergey Levine. Model-agnostic meta-learning for fast adap-
435 tation of deep networks. In *International conference on machine learning*, pages 1126–1135.
436 PMLR, 2017.
- 437 [21] Luis Antonio Galárraga, Christina Teflioudi, Katja Hose, and Fabian Suchanek. Amie: associa-
438 tion rule mining under incomplete evidence in ontological knowledge bases. In *Proceedings of*
439 *the 22nd international conference on World Wide Web*, pages 413–422, 2013.
- 440 [22] Mikhail Galkin, Etienne Denis, Jiapeng Wu, and William L Hamilton. Nodepiece: Composi-
441 tional and parameter-efficient representations of large knowledge graphs. In *International*
442 *Conference on Learning Representations*, 2021.
- 443 [23] Mikhail Galkin, Zhaocheng Zhu, Hongyu Ren, and Jian Tang. Inductive logical query answering
444 in knowledge graphs. In Alice H. Oh, Alekh Agarwal, Danielle Belgrave, and Kyunghyun Cho,
445 editors, *Advances in Neural Information Processing Systems*, 2022.
- 446 [24] Yuxia Geng, Jiaoyan Chen, Zhuo Chen, Jeff Z. Pan, Zhiquan Ye, Zonggang Yuan, Yantao Jia,
447 and Huajun Chen. Ontozsl: Ontology-enhanced zero-shot learning. In Jure Leskovec, Marko
448 Grobelnik, Marc Najork, Jie Tang, and Leila Zia, editors, *WWW '21: The Web Conference 2021,*
449 *Virtual Event / Ljubljana, Slovenia, April 19-23, 2021*, pages 3325–3336. ACM / IW3C2, 2021.
- 450 [25] Yuxia Geng, Jiaoyan Chen, Jeff Z Pan, Mingyang Chen, Song Jiang, Wen Zhang, and Huajun
451 Chen. Relational message passing for fully inductive knowledge graph completion. In *2023*
452 *IEEE 39th International Conference on Data Engineering (ICDE)*, pages 1221–1233. IEEE,
453 2023.
- 454 [26] Genet Asefa Gesese, Harald Sack, and Mehwish Alam. Raild: Towards leveraging relation fea-
455 tures for inductive link prediction in knowledge graphs. In *Proceedings of the 11th International*
456 *Joint Conference on Knowledge Graphs*, pages 82–90, 2022.
- 457 [27] Justin Gilmer, Samuel S. Schoenholz, Patrick F. Riley, Oriol Vinyals, and George E. Dahl.
458 Neural message passing for quantum chemistry. In *Proceedings of the 34th International*
459 *Conference on Machine Learning*, volume 70 of *Proceedings of Machine Learning Research*,
460 pages 1263–1272. PMLR, 2017.
- 461 [28] Xavier Glorot and Yoshua Bengio. Understanding the difficulty of training deep feedfor-
462 ward neural networks. In *Proceedings of the thirteenth international conference on artificial*
463 *intelligence and statistics*, pages 249–256. JMLR Workshop and Conference Proceedings, 2010.
- 464 [29] Ian J. Goodfellow, Jonathon Shlens, and Christian Szegedy. Explaining and harnessing adver-
465 sarial examples. In *International Conference on Learning Representations (ICLR)*, 2015.
- 466 [30] Will Hamilton, Zhitao Ying, and Jure Leskovec. Inductive representation learning on large
467 graphs. *Advances in neural information processing systems*, 30, 2017.
- 468 [31] Qian Huang, Hongyu Ren, and Jure Leskovec. Few-shot relational reasoning via connection
469 subgraph pretraining. In *Neural Information Processing Systems*, 2022.
- 470 [32] Dora Jambor, Komal Teru, Joelle Pineau, and William L Hamilton. Exploring the limits of
471 few-shot link prediction in knowledge graphs. *arXiv preprint arXiv:2102.03419*, 2021.
- 472 [33] Thomas Kipf and Max Welling. Semi-supervised classification with graph convolutional
473 networks. In *International Conference on Learning Representations*, 2017.
- 474 [34] Ni Lao and William W Cohen. Relational retrieval using a combination of path-constrained
475 random walks. *Machine learning*, 81(1):53–67, 2010.
- 476 [35] Jaejun Lee, Chanyoung Chung, and Joyce Jiyoung Whang. InGram: Inductive knowledge
477 graph embedding via relation graphs. In *Proceedings of the 40th International Conference on*
478 *Machine Learning*, pages 18796–18809, 2023.

- 479 [36] Jens Lehmann, Robert Isele, Max Jakob, Anja Jentzsch, Dimitris Kontokostas, Pablo N Mendes,
480 Sebastian Hellmann, Mohamed Morsey, Patrick Van Kleef, Sören Auer, et al. Dbpedia—a large-
481 scale, multilingual knowledge base extracted from wikipedia. *Semantic web*, 6(2):167–195,
482 2015.
- 483 [37] Jure Leskovec and Christos Faloutsos. Sampling from large graphs. In *Proceedings of the 12th*
484 *ACM SIGKDD International Conference on Knowledge Discovery and Data Mining*, KDD '06,
485 page 631–636, New York, NY, USA, 2006. Association for Computing Machinery.
- 486 [38] Xin Lv, Yuxian Gu, Xu Han, Lei Hou, Juanzi Li, and Zhiyuan Liu. Adapting meta knowledge
487 graph information for multi-hop reasoning over few-shot relations. In *Proceedings of the 2019*
488 *Conference on Empirical Methods in Natural Language Processing and the 9th International*
489 *Joint Conference on Natural Language Processing (EMNLP-IJCNLP)*, pages 3376–3381, 2019.
- 490 [39] Haggai Maron, Or Litany, Gal Chechik, and Ethan Fetaya. On learning sets of symmetric
491 elements. In *International Conference on Machine Learning*, pages 6734–6744. PMLR, 2020.
- 492 [40] Christian Meilicke, Manuel Fink, Yanjie Wang, Daniel Ruffinelli, Rainer Gemulla, and Heiner
493 Stuckenschmidt. Fine-grained evaluation of rule-and embedding-based systems for knowledge
494 graph completion. In *International semantic web conference*, pages 3–20. Springer, 2018.
- 495 [41] Christopher Morris, Martin Ritzert, Matthias Fey, William L. Hamilton, Jan Eric Lenssen,
496 Gaurav Rattan, and Martin Grohe. Weisfeiler and leman go neural: Higher-order graph neural
497 networks. *Proceedings of the AAAI Conference on Artificial Intelligence*, 33(01):4602–4609,
498 Jul. 2019.
- 499 [42] Ryan Murphy, Balasubramaniam Srinivasan, Vinayak Rao, and Bruno Ribeiro. Relational
500 pooling for graph representations. In *International Conference on Machine Learning*, pages
501 4663–4673. PMLR, 2019.
- 502 [43] Ryan Murphy, Balasubramaniam Srinivasan, Vinayak Rao, and Bruno Ribeiro. Relational
503 pooling for graph representations. In *Proceedings of the 36th International Conference on*
504 *Machine Learning*, 2019.
- 505 [44] Maximilian Nickel, Lorenzo Rosasco, and Tomaso Poggio. Holographic embeddings of
506 knowledge graphs. In *Proceedings of the AAAI Conference on Artificial Intelligence*, volume 30,
507 2016.
- 508 [45] Maximilian Nickel, Volker Tresp, and Hans-Peter Kriegel. A three-way model for collective
509 learning on multi-relational data. In *Icml*, 2011.
- 510 [46] Pengda Qin, Xin Wang, Wenhui Chen, Chunyun Zhang, Weiran Xu, and William Yang Wang.
511 Generative adversarial zero-shot relational learning for knowledge graphs. In *Proceedings of*
512 *the AAAI Conference on Artificial Intelligence*, volume 34, pages 8673–8680, 2020.
- 513 [47] Haiquan Qiu, Yongqi Zhang, Yong Li, and Quanming Yao. Logical expressiveness of graph
514 neural network for knowledge graph reasoning. *arXiv preprint arXiv:2303.12306*, 2023.
- 515 [48] Thomas Rebele, Fabian Suchanek, Johannes Hoffart, Joanna Biega, Erdal Kuzey, and Gerhard
516 Weikum. Yago: A multilingual knowledge base from wikipedia, wordnet, and geonames. In
517 *The Semantic Web—ISWC 2016: 15th International Semantic Web Conference, Kobe, Japan,*
518 *October 17–21, 2016, Proceedings, Part II 15*, pages 177–185. Springer, 2016.
- 519 [49] Benedek Rozemberczki, Oliver Kiss, and Rik Sarkar. Little Ball of Fur: A Python Library for
520 Graph Sampling. In *Proceedings of the 29th ACM International Conference on Information*
521 *and Knowledge Management (CIKM '20)*, page 3133–3140. ACM, 2020.
- 522 [50] Daniel Ruffinelli, Samuel Broscheit, and Rainer Gemulla. You can teach an old dog new
523 tricks! on training knowledge graph embeddings. In *International Conference on Learning*
524 *Representations*, 2020.
- 525 [51] Ali Sadeghian, Mohammadreza Armandpour, Patrick Ding, and Daisy Zhe Wang. Drum:
526 End-to-end differentiable rule mining on knowledge graphs. *Advances in Neural Information*
527 *Processing Systems*, 32, 2019.
- 528 [52] Ryoma Sato, Makoto Yamada, and Hisashi Kashima. Random features strengthen graph neural
529 networks. In *Proceedings of the 2021 SIAM international conference on data mining (SDM)*,
530 pages 333–341. SIAM, 2021.

- 531 [53] Michael Schlichtkrull, Thomas N Kipf, Peter Bloem, Rianne van den Berg, Ivan Titov, and Max
532 Welling. Modeling relational data with graph convolutional networks. In *European semantic*
533 *web conference*, pages 593–607. Springer, 2018.
- 534 [54] Balasubramaniam Srinivasan and Bruno Ribeiro. On the equivalence between positional
535 node embeddings and structural graph representations. In *Eighth International Conference on*
536 *Learning Representations*, 2020.
- 537 [55] Zequn Sun, Wei Hu, Qingheng Zhang, and Yuzhong Qu. Bootstrapping entity alignment with
538 knowledge graph embedding. In *IJCAI*, volume 18, 2018.
- 539 [56] Zequn Sun, Chengming Wang, Wei Hu, Muhao Chen, Jian Dai, Wei Zhang, and Yuzhong
540 Qu. Knowledge graph alignment network with gated multi-hop neighborhood aggregation.
541 In *Proceedings of the AAAI Conference on Artificial Intelligence*, volume 34, pages 222–229,
542 2020.
- 543 [57] Zequn Sun, Qingheng Zhang, Wei Hu, Chengming Wang, Muhao Chen, Farahnaz Akrami,
544 and Chengkai Li. A benchmarking study of embedding-based entity alignment for knowledge
545 graphs. *Proceedings of the VLDB Endowment*, 13(11):2326–2340, 2020.
- 546 [58] Zhiqing Sun, Zhi-Hong Deng, Jian-Yun Nie, and Jian Tang. Rotate: Knowledge graph em-
547 bedding by relational rotation in complex space. In *International Conference on Learning*
548 *Representations*, 2019.
- 549 [59] Ilya Sutskever, Joshua Tenenbaum, and Russ R Salakhutdinov. Modelling relational data using
550 bayesian clustered tensor factorization. *Advances in neural information processing systems*, 22,
551 2009.
- 552 [60] Komal Teru, Etienne Denis, and Will Hamilton. Inductive relation prediction by subgraph
553 reasoning. In *International Conference on Machine Learning*, pages 9448–9457. PMLR, 2020.
- 554 [61] Kristina Toutanova and Danqi Chen. Observed versus latent features for knowledge base and
555 text inference. In *Proceedings of the 3rd workshop on continuous vector space models and their*
556 *compositionality*, pages 57–66, 2015.
- 557 [62] T Trouillon, CR Dance, E Gaussier, J Welbl, S Riedel, and G Bouchard. Knowledge graph
558 completion via complex tensor factorization. *Journal of Machine Learning Research*, 18(130):1–
559 38, 2017.
- 560 [63] Théo Trouillon, Johannes Welbl, Sebastian Riedel, Éric Gaussier, and Guillaume Bouchard.
561 Complex embeddings for simple link prediction. In *International conference on machine*
562 *learning*, pages 2071–2080. PMLR, 2016.
- 563 [64] Petar Veličković, Guillem Cucurull, Arantxa Casanova, Adriana Romero, Pietro Lio, and Yoshua
564 Bengio. Graph attention networks. *arXiv preprint arXiv:1710.10903*, 2017.
- 565 [65] Petar Veličković, Guillem Cucurull, Arantxa Casanova, Adriana Romero, Pietro Lio, and Yoshua
566 Bengio. Graph attention networks. *ICLR*, 2018.
- 567 [66] Denny Vrandečić and Markus Krötzsch. Wikidata: a free collaborative knowledgebase. *Com-*
568 *munications of the ACM*, 57(10):78–85, 2014.
- 569 [67] Hongwei Wang, Hongyu Ren, and Jure Leskovec. Relational message passing for knowledge
570 graph completion. In *Proceedings of the 27th ACM SIGKDD Conference on Knowledge*
571 *Discovery & Data Mining*, pages 1697–1707, 2021.
- 572 [68] Xiaozhi Wang, Tianyu Gao, Zhaocheng Zhu, Zhengyan Zhang, Zhiyuan Liu, Juanzi Li, and
573 Jian Tang. Kepler: A unified model for knowledge embedding and pre-trained language
574 representation. *Transactions of the Association for Computational Linguistics*, 9:176–194,
575 2021.
- 576 [69] Zhen Wang, Jianwen Zhang, Jianlin Feng, and Zheng Chen. Knowledge graph embedding by
577 translating on hyperplanes. In *Proceedings of the AAAI conference on artificial intelligence*,
578 volume 28, 2014.
- 579 [70] Zhichun Wang, Qingsong Lv, Xiaohan Lan, and Yu Zhang. Cross-lingual knowledge graph
580 alignment via graph convolutional networks. In *Proceedings of the 2018 conference on empirical*
581 *methods in natural language processing*, pages 349–357, 2018.
- 582 [71] Wei Wei, Chao Huang, Lianghao Xia, Yong Xu, Jiashu Zhao, and Dawei Yin. Contrastive meta
583 learning with behavior multiplicity for recommendation. In *Proceedings of the fifteenth ACM*
584 *international conference on web search and data mining*, pages 1120–1128, 2022.

- 585 [72] Wenhan Xiong, Mo Yu, Shiyu Chang, Xiaoxiao Guo, and William Yang Wang. One-shot
586 relational learning for knowledge graphs. In *Proceedings of the 2018 Conference on Empirical*
587 *Methods in Natural Language Processing*, pages 1980–1990, 2018.
- 588 [73] Keyulu Xu, Weihua Hu, Jure Leskovec, and Stefanie Jegelka. How powerful are graph neural
589 networks? In *International Conference on Learning Representations*, 2019.
- 590 [74] Kun Xu, Liwei Wang, Mo Yu, Yansong Feng, Yan Song, Zhiguo Wang, and Dong Yu. Cross-
591 lingual knowledge graph alignment via graph matching neural network. In *Annual Meeting*
592 *of the Association for Computational Linguistics*. Association for Computational Linguistics
593 (ACL), 2019.
- 594 [75] Yuchen Yan, Lihui Liu, Yikun Ban, Baoyu Jing, and Hanghang Tong. Dynamic knowledge
595 graph alignment. In *Proceedings of the AAAI Conference on Artificial Intelligence*, volume 35,
596 pages 4564–4572, 2021.
- 597 [76] Bishan Yang, Scott Wen-tau Yih, Xiaodong He, Jianfeng Gao, and Li Deng. Embedding entities
598 and relations for learning and inference in knowledge bases. In *Proceedings of the International*
599 *Conference on Learning Representations (ICLR) 2015*, 2015.
- 600 [77] Fan Yang, Zhilin Yang, and William W Cohen. Differentiable learning of logical rules for
601 knowledge base reasoning. *Advances in neural information processing systems*, 30, 2017.
- 602 [78] Jiaxuan You, Rex Ying, and Jure Leskovec. Position-aware graph neural networks. In *International*
603 *conference on machine learning*, pages 7134–7143. PMLR, 2019.
- 604 [79] Xiao Yu, Xiang Ren, Yizhou Sun, Bradley Sturt, Urvashi Khandelwal, Quanquan Gu, Brandon
605 Norick, and Jiawei Han. Recommendation in heterogeneous information networks with implicit
606 user feedback. In *Proceedings of the 7th ACM conference on Recommender systems*, pages
607 347–350, 2013.
- 608 [80] Manzil Zaheer, Satwik Kottur, Siamak Ravanbakhsh, Barnabas Poczos, Russ R Salakhutdinov,
609 and Alexander J Smola. Deep sets. In *Advances in neural information processing systems*,
610 pages 3391–3401, 2017.
- 611 [81] Hanwen Zha, Zhiyu Chen, and Xifeng Yan. Inductive relation prediction by bert. *Proceedings*
612 *of the AAAI Conference on Artificial Intelligence*, 36:5923–5931, Jun. 2022.
- 613 [82] Chuxu Zhang, Huaxiu Yao, Chao Huang, Meng Jiang, Zhenhui Li, and Nitesh V Chawla.
614 Few-shot knowledge graph completion. In *Proceedings of the AAAI conference on artificial*
615 *intelligence*, volume 34, pages 3041–3048, 2020.
- 616 [83] Muhan Zhang and Yixin Chen. Link prediction based on graph neural networks. *Advances in*
617 *neural information processing systems*, 31, 2018.
- 618 [84] Muhan Zhang, Pan Li, Yinglong Xia, Kai Wang, and Long Jin. Labeling trick: A theory of using
619 graph neural networks for multi-node representation learning. *Advances in Neural Information*
620 *Processing Systems*, 34:9061–9073, 2021.
- 621 [85] Ming Zhao, Weijia Jia, and Yusheng Huang. Attention-based aggregation graph networks for
622 knowledge graph information transfer. In *Advances in Knowledge Discovery and Data Mining:*
623 *24th Pacific-Asia Conference, PAKDD 2020, Singapore, May 11–14, 2020, Proceedings, Part II*
624 *24*, pages 542–554. Springer, 2020.
- 625 [86] Zhaocheng Zhu, Mikhail Galkin, Zuobai Zhang, and Jian Tang. Neural-symbolic models for
626 logical queries on knowledge graphs. In *International Conference on Machine Learning*, pages
627 27454–27478. PMLR, 2022.
- 628 [87] Zhaocheng Zhu, Zuobai Zhang, Louis-Pascal Xhonneux, and Jian Tang. Neural bellman-ford
629 networks: A general graph neural network framework for link prediction. *Advances in Neural*
630 *Information Processing Systems*, 34:29476–29490, 2021.

631 A Additional example for doubly inductive link prediction

632 This example depicts an even harder scenario than the example in Figure 1, obtained from a fictional alien civilization.
 633
 634
 635 Knowing nothing about alien languages, we note that in training, all adjacent relations are different. Minimally, we could
 636
 637 predict the missing relation in red in test data is not “ \neq ”. By introducing equivariance in relations, it is possible for a model
 638
 639 to predict relation types uniformly over the set of other $(R-1)$ relations except for the existing relation “ \neq ”, which is all we know about the
 640
 641
 642
 643 aliens.

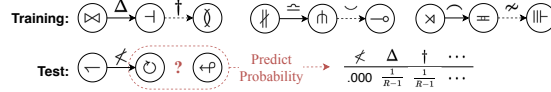


Figure 4: **Alien discrete attributed multigraph:** The task is to predict the missing relation “?” in red. Training only tells us that relations do not repeat in a path.

644 B Connection to Double Equivariant Logical Reasoning

645 In what follows, we follow the literature and connect link prediction in discrete attributed multigraph
 646 to logical induction [60, 86, 47]. Existing logical induction requires all involved relations to be
 647 observed at least once, thus, such logical reasoning can not generalize to new relation types. We
 648 propose the Universally Quantified Entity and Relation (UQER) Horn clause, a double equivariant
 649 extension of conventional logical reasoning, which is capable of generalizing to new relation types,
 650 and show that the double invariant triplet representation in Definition 2.4 is capable of encoding such
 651 set of UQER Horn Clauses.

652 **Definition B.1** (Universally Quantified Entity and Relation (UQER) Horn clause). An UQER Horn
 653 clause involving M nodes and K relations is defined by an indicator tensor $\mathbf{B} \in \{0, 1\}^{M \times K \times M}$:

$$\forall E_1 \in \mathcal{V}^{(*)}, \left(\forall E_u \in \mathcal{V}^{(*)} \setminus \{E_1, \dots, E_{u-1}\} \right)_{u=2}^M, \forall C_1 \in \mathcal{R}^{(*)}, \left(\forall C_c \in \mathcal{R}^{(*)} \setminus \{C_1, \dots, C_{c-1}\} \right)_{c=2}^K, \\ \bigwedge_{\substack{u, u'=1, \dots, M, c=1, \dots, K, \\ \mathbf{B}_{u, c, u'}=1}} (E_u, C_c, E_{u'}) \implies (E_1, C_1, E_h), \quad (5)$$

654 for any node set $\mathcal{V}^{(*)}$ and relation set $\mathcal{R}^{(*)}$ with number of nodes and relations $N^{(*)}, R^{(*)}$ s.t.
 655 $N^{(*)} \geq M, R^{(*)} \geq K, h \in \{1, 2\}$ (where $h = 1$ indicates a self-loop relation or a relational node
 656 attribute), where if $M > h, \forall u \in \{h+1, \dots, M\}, \sum_{u'=1}^M \sum_{c=1}^K \mathbf{B}_{u, c, u'} + \mathbf{B}_{u', c, u} \geq 1$, and if
 657 $K \geq 2, \forall c \in \{2, \dots, K\}, \sum_{u=1}^M \sum_{u'=1}^M \mathbf{B}_{u, c, u'} + \mathbf{B}_{u', c, u} \geq 1$ (every variable should appear at least
 658 once in the formula).

659 Note that our definition of UQER Horn clauses (Definition B.1) is a generalization of the First Order
 660 Logic (FOL) clauses in [77, 40, 51, 60] such that the relations in the Horn clauses are also universally
 661 quantified rather than predefined constants. UQER can be used to predict new relations in the test
 662 attributed multigraph with *pattern matching*, i.e., if the left-hand-side (condition) of a UQER can
 663 be satisfied in the test attributed multigraph, then the right-hand-side (implication) triplet should be
 664 present. In Figure 5, we illustrate two examples using UQER to predict new relations at test time.

665 We now connect our double equivariant representations (Definition 2.3) with the UQER Horn clauses.

666 **Theorem B.2.** For any UQER Horn clause defined by $\mathbf{B} \in \{0, 1\}^{M \times K \times M}$ (Definition B.1),
 667 there exists a double invariant triplet predictor $\Gamma_{tri} : \cup_{N=1}^{\infty} \cup_{R=2}^{\infty} ([N] \times [R] \times [N]) \times$
 668 $\mathbb{A} \rightarrow \{0, 1\}$ (Definition 2.3), such that for any set of truth statements $\mathcal{S} \subseteq \mathcal{V}^{(*)} \times$
 669 $\mathcal{R}^{(*)} \times \mathcal{V}^{(*)}$ and their equivalent tensor representation $\mathbf{A}^{(*)} \in \mathbb{A}$ (where $\mathbf{A}_{i, k, j}^{(*)} =$
 670 1 iff $(v_i^{(*)}, r_k^{(*)}, v_j^{(*)}) \in \mathcal{S}$), it satisfies $\Gamma_{tri}((i, k, j), \mathbf{A}^{(*)}) = 1$ iff $(i, k, j) \in \mathcal{S}'$, where
 671 $\mathcal{S}' = \{(i, k, j) \mid \forall (i, k, j), \text{ such that } (E_1, C_1, E_2) = (v_i^{(*)}, r_k^{(*)}, v_j^{(*)}) \in \mathcal{V}^{(*)} \times \mathcal{R}^{(*)} \times$
 672 $\mathcal{V}^{(*)}, \exists^{M-2} E_3, \dots, E_M \in \mathcal{V}^{(*)} \setminus \{E_1, E_2\}, \exists^{K-1} C_2, \dots, C_K \in \mathcal{R}^{(*)} \setminus \{C_1\}, \text{ where } \forall (u, c, u') \in$
 673 $[M] \times [K] \times [M], \mathbf{B}_{u, c, u'} = 1 \implies (E_u, C_c, E_{u'}) \in \mathcal{S}\}$ is the set of true statements induced by *modus*
 674 *ponens* by the truth statements \mathcal{S} and the UQER Horn clause, where the existential quantifier \exists^k
 675 means exists at least k distinct values.
 676

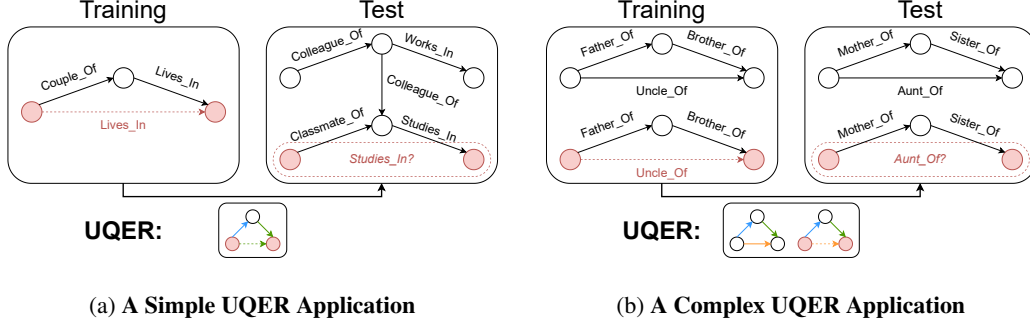


Figure 5: (a) The UQER (bottom) learned from training can be used to predict missing new relation “Studies_In” in red since an assignment of left-hand-side of the UQER ($E_1, \text{Classmate_Of}, E_3$) \wedge ($E_3, \text{Studies_In}, E_2$) is satisfied in test. (b) UQER can contain disconnected components, giving more freedom to its application. For example, the UQER (bottom) can be learned from training to repeat arbitrary logical chain, which makes it possible to deal with new female relations at test time and will predict “Aunt_Of” in test just as “Uncle_Of” (red) in training.

677 The full proof is in Appendix C, showing how the universal quantification in Definition B.1 is a
 678 double invariant predictor.

679 C Proofs

680 **Theorem 2.6.** For all $\mathbf{A}^{(*)} \in \mathbb{A}$ with number of nodes and relations $N^{(*)}, R^{(*)}$, given a double
 681 invariant triplet representation Γ_{tri} , we can construct a double equivariant graph representation as
 682 $(\Gamma_{\text{gra}}(\mathbf{A}^{(*)}))_{i,k,j} := \Gamma_{\text{tri}}((i, k, j), \mathbf{A}^{(*)}), \forall (i, k, j) \in [N^{(*)}] \times [R^{(*)}] \times [N^{(*)}]$, and vice-versa.

683 *Proof.* (\Rightarrow) For any discrete attributed multigraph $\mathbf{A}^{(*)} \in \mathbb{A}$ with number of nodes and rela-
 684 tions $N^{(*)}, R^{(*)}$, $\Gamma_{\text{tri}} : \cup_{N=1}^{\infty} \cup_{R=2}^{\infty} ([N] \times [R] \times [N]) \times \mathbb{A} \rightarrow \mathbb{R}^d, d \geq 1$ is a double in-
 685 variant triplet representation as in Definition 2.3. Using the double invariant triplet represen-
 686 tation, we can define a function $\Gamma_{\text{gra}} : \mathbb{A} \rightarrow \cup_{N=1}^{\infty} \cup_{R=2}^{\infty} \mathbb{R}^{N \times R \times N \times d}$ such that $\forall (i, k, j) \in$
 687 $[N^{(*)}] \times [R^{(*)}] \times [N^{(*)}]$, $(\Gamma_{\text{gra}}(\mathbf{A}^{(*)}))_{i,k,j} := \Gamma_{\text{tri}}((i, k, j), \mathbf{A}^{(*)})$. Then $\forall \phi \in \mathbb{S}_{N^{(*)}}, \forall \tau \in$
 688 $\mathbb{S}_{R^{(*)}}$, $(\Gamma_{\text{gra}}(\phi \circ \tau \circ \mathbf{A}^{(*)}))_{\phi \circ i, \tau \circ k, \phi \circ j} := \Gamma_{\text{tri}}((\phi \circ i, \tau \circ k, \phi \circ j), \phi \circ \tau \circ \mathbf{A}^{(*)})$. We know
 689 $\Gamma_{\text{tri}}((i, k, j), \mathbf{A}^{(*)}) = \Gamma_{\text{tri}}((\phi \circ i, \tau \circ k, \phi \circ j), \phi \circ \tau \circ \mathbf{A}^{(*)})$. Thus we conclude, $\forall \phi \in \mathbb{S}_{N^{(*)}}, \forall \tau \in$
 690 $\mathbb{S}_{R^{(*)}}, \forall (i, k, j) \in [N^{(*)}] \times [R^{(*)}] \times [N^{(*)}]$, $(\phi \circ \tau \circ \Gamma_{\text{gra}}(\mathbf{A}^{(*)}))_{\phi \circ i, \tau \circ k, \phi \circ j} := (\Gamma_{\text{gra}}(\mathbf{A}^{(*)}))_{i,k,j} :=$
 691 $\Gamma_{\text{tri}}((i, k, j), \mathbf{A}^{(*)}) = \Gamma_{\text{tri}}((\phi \circ i, \tau \circ k, \phi \circ j), \phi \circ \tau \circ \mathbf{A}^{(*)}) = (\Gamma_{\text{gra}}(\phi \circ \tau \circ \mathbf{A}^{(*)}))_{\phi \circ i, \tau \circ k, \phi \circ j}$. In
 692 conclusion, we show that $\phi \circ \tau \circ \Gamma_{\text{gra}}(\mathbf{A}^{(*)}) = \Gamma_{\text{gra}}(\phi \circ \tau \circ \mathbf{A}^{(*)})$, which proves the constructed Γ_{gra}
 693 is a double equivariant representation as in Definition 2.5.

694 (\Leftarrow) For any discrete attributed multigraph $\mathbf{A}^{(*)} \in \mathbb{A}$ with number of nodes and relations $N^{(*)}, R^{(*)}$,
 695 assume $\Gamma_{\text{gra}} : \mathbb{A} \rightarrow \cup_{N=1}^{\infty} \cup_{R=2}^{\infty} \mathbb{R}^{N \times R \times N \times d}$ is a double equivariant representation as Definition 2.5.
 696 Since $\Gamma_{\text{gra}}(\phi \circ \tau \circ \mathbf{A}^{(*)}) = \phi \circ \tau \circ \Gamma_{\text{gra}}(\mathbf{A}^{(*)})$, then $\forall (i, k, j) \in [N^{(*)}] \times [R^{(*)}] \times [N^{(*)}]$, $(\Gamma_{\text{gra}}(\phi \circ$
 697 $\tau \circ \mathbf{A}^{(*)}))_{\phi \circ i, \tau \circ k, \phi \circ j} = (\phi \circ \tau \circ \Gamma_{\text{gra}}(\mathbf{A}^{(*)}))_{\phi \circ i, \tau \circ k, \phi \circ j} = (\Gamma_{\text{gra}}(\mathbf{A}^{(*)}))_{i,k,j}$. Then we can define
 698 $\Gamma_{\text{tri}} : \cup_{N=1}^{\infty} \cup_{R=2}^{\infty} ([N] \times [R] \times [N]) \times \mathbb{A} \rightarrow \mathbb{R}^d, d \geq 1$, such that $\forall (i, k, j) \in [N^{(*)}] \times [R^{(*)}] \times [N^{(*)}]$,
 699 $\Gamma_{\text{tri}}((i, k, j), \mathbf{A}^{(*)}) = (\Gamma_{\text{gra}}(\mathbf{A}^{(*)}))_{i,k,j}$. It is clear that $\Gamma_{\text{tri}}((i, k, j), \mathbf{A}^{(*)}) = (\Gamma_{\text{gra}}(\mathbf{A}^{(*)}))_{i,k,j} =$
 700 $(\Gamma_{\text{gra}}(\phi \circ \tau \circ \mathbf{A}^{(*)}))_{\phi \circ i, \tau \circ k, \phi \circ j} = \Gamma_{\text{tri}}((\phi \circ i, \tau \circ k, \phi \circ j), \phi \circ \tau \circ \mathbf{A}^{(*)})$. Thus, we show Γ_{tri} is a
 701 double invariant triplet representation as in Definition 2.3. \square

702 **Theorem 2.8** (From distributional double equivariant positional embeddings to double equivariant
 703 representations). For any attributed multigraph $\mathbf{A}^{(*)} \in \mathbb{A}$, the average $\mathbb{E}_p(\mathbf{Z} | \mathbf{A}^{(*)})[\mathbf{Z} | \mathbf{A}^{(*)}]$ is a
 704 double equivariant attributed multigraph representation (Definition 2.5) for any distributional double
 705 equivariant positional embeddings $\mathbf{Z} | \mathbf{A}^{(*)}$ (Definition 2.7).

706 *Proof.* Based on Definition 2.7, for any attributed multigraph $\mathbf{A}^{(*)} \in \mathbb{A}$ with number of nodes
 707 and relations $N^{(*)}, R^{(*)}$, the distributionally double equivariant positional embeddings of $\mathbf{A}^{(*)}$ are

708 defined as joint samples of random variables $\mathbf{Z}|\mathbf{A}^{(*)} \sim p(\mathbf{Z}|\mathbf{A}^{(*)})$, where the tensor \mathbf{Z} is defined
709 as $\mathbf{z}_{i,k,j} \in \mathbb{R}^d$, $d \geq 1$, $\forall(i, k, j) \in [N^{(*)}] \times [R^{(*)}] \times [N^{(*)}]$, where we say $p(\mathbf{Z}|\mathbf{A}^{(*)})$ is a double
710 equivariant probability distribution on $\mathbf{A}^{(*)}$ defined as $\forall\phi \in \mathbb{S}_{N^{(*)}}, \forall\tau \in \mathbb{S}_{R^{(*)}}, p(\mathbf{Z}|\mathbf{A}^{(*)}) =$
711 $p(\phi \circ \tau \circ \mathbf{Z}|\phi \circ \tau \circ \mathbf{A}^{(*)})$.

712 The tensor \mathbf{Z} is defined as $\mathbf{z}_{i,k,j} \in \mathbb{R}^d, \forall(i, k, j) \in [N^{(*)}] \times [R^{(*)}] \times [N^{(*)}]$, thus $\mathbf{Z} \in$
713 $\mathbb{R}^{N^{(*)} \times R^{(*)} \times N^{(*)} \times d}$. So we can consider $\mathbb{E}_{p(\mathbf{Z}|\mathbf{A}^{(*)})}[\mathbf{Z}|\mathbf{A}^{(*)}]$ as a function on $\mathbf{A}^{(*)}$, and output a repre-
714 sentation in $\mathbb{R}^{N^{(*)} \times R^{(*)} \times N^{(*)} \times d}$. Since $\forall\phi \in \mathbb{S}_{N^{(*)}}, \forall\tau \in \mathbb{S}_{R^{(*)}}, p(\mathbf{Z}|\mathbf{A}^{(*)}) = p(\phi \circ \tau \circ \mathbf{Z}|\phi \circ \tau \circ \mathbf{A}^{(*)})$,
715 it is clear to have $\forall\phi \in \mathbb{S}_{N^{(*)}}, \forall\tau \in \mathbb{S}_{R^{(*)}}, \phi \circ \tau \circ \mathbb{E}_{p(\mathbf{Z}|\mathbf{A}^{(*)})}[\mathbf{Z}|\mathbf{A}^{(*)}] = \phi \circ \tau \circ \int \mathbf{z}p(\mathbf{Z} = \mathbf{z}|\mathbf{A}^{(*)})d\mathbf{z} =$
716 $\int \phi \circ \tau \circ \mathbf{z}p(\mathbf{Z} = \mathbf{z}|\mathbf{A}^{(*)})d\mathbf{z} = \int \phi \circ \tau \circ \mathbf{z}p(\phi \circ \tau \circ \mathbf{Z} = \phi \circ \tau \circ \mathbf{z}|\phi \circ \tau \circ \mathbf{A}^{(*)})d(\phi \circ \tau \circ \mathbf{z}) =$
717 $\mathbb{E}_{p(\phi \circ \tau \circ \mathbf{Z}|\phi \circ \tau \circ \mathbf{A}^{(*)})}[\phi \circ \tau \circ \mathbf{Z}|\phi \circ \tau \circ \mathbf{A}^{(*)}]$. Since the permutation ϕ, τ only changes the ordering of
718 the output representation element-wise, we can interchange the permutations with the integral.

719 Finally, for any attributed multigraph $\mathbf{A}^{(*)} \in \mathbb{A}$ with number of nodes and relations $N^{(*)}, R^{(*)}$,
720 we can define $\Gamma_{\text{gra}}(\mathbf{A}^{(*)}) : \mathbb{A} \rightarrow \cup_{N=1}^{\infty} \cup_{R=2}^{\infty} \mathbb{R}^{N \times R \times N \times d}, d \geq 1$ such that $\Gamma_{\text{gra}}(\mathbf{A}^{(*)}) :=$
721 $\mathbb{E}_{p(\mathbf{Z}|\mathbf{A}^{(*)})}[\mathbf{Z}|\mathbf{A}^{(*)}]$. And we can derive $\phi \circ \tau \circ \Gamma_{\text{gra}}(\mathbf{A}^{(*)}) = \phi \circ \tau \circ \mathbb{E}_{p(\mathbf{Z}|\mathbf{A}^{(*)})}[\mathbf{Z}|\mathbf{A}^{(*)}] =$
722 $\mathbb{E}_{p(\phi \circ \tau \circ \mathbf{Z}|\phi \circ \tau \circ \mathbf{A}^{(*)})}[\phi \circ \tau \circ \mathbf{Z}|\phi \circ \tau \circ \mathbf{A}^{(*)}] = \Gamma_{\text{gra}}(\phi \circ \tau \circ \mathbf{A}^{(*)})$. Thus, $\Gamma_{\text{gra}}(\mathbf{A}^{(*)}) := \mathbb{E}_{p(\mathbf{Z}|\mathbf{A}^{(*)})}[\mathbf{Z}|\mathbf{A}^{(*)}]$
723 is a double equivariant attributed multigraph representation as per Definition 2.5. \square

724 **Lemma 3.1.** Γ_{ISDEA} in Equation (2) is a double invariant triplet representation as per Definition 2.3.

725 *Proof.* From our model architecture (Equation (2)), $\Gamma_{\text{ISDEA}}((i, k, j), \mathbf{A}^{(*)}) = (h_{i,k}^{(T)} \| h_{j,k}^{(T)} \| d(i, j) \|$
726 $d(j, i))$. Using DSS layers, we can guarantee the node representations $h_{i,k}^{(T)}$ we learn are double
727 invariant under the node and relation permutations, where $h_{i,k}^{(T)}$ in $\mathbf{A}^{(*)}$ is equal to $h_{\phi \circ i, \tau \circ k}^{(T)}$ in
728 $\phi \circ \tau \circ \mathbf{A}^{(*)}$. It is also clear that the distance function is invariant to node and relation permu-
729 tations, i.e. $\forall i, j \in [N^{(*)}], d(i, j)$ in $\mathbf{A}^{(*)}$ is the same as $d(\phi \circ i, \phi \circ j)$ in $\phi \circ \tau \circ \mathbf{A}^{(*)}$. Thus
730 $\Gamma_{\text{ISDEA}}((i, k, j), \mathbf{A}^{(*)}) = \Gamma_{\text{ISDEA}}((\phi \circ i, \tau \circ k, \phi \circ j), \phi \circ \tau \circ \mathbf{A}^{(*)})$ is a double invariant triplet
731 representation as in Definition 2.5. \square

732 **Lemma 3.2.** The triplet representations generated by InGram [35] output distributionally double
733 equivariant positional embeddings (Definition 2.7).

734 *Proof.* To solve doubly inductive link prediction, InGram [35] first constructs a *relation graph*, in
735 which the relation types are treated as nodes, and the edges between them are weighted by the affinity
736 scores, a measure of co-occurrence between relation types in the original attributed multigraph.
737 It then employs a variant of the GATv2 [65, 6] on the relation graph to propagate and generate
738 embeddings for the relation types. These relation embeddings, together with another GATv2, are
739 applied to the original attributed multigraph to generate embeddings for the nodes. Finally, a variant
740 of DistMult [76] is used to compute the scores for individual triplets from the embeddings of the
741 head and tail nodes and the embedding of the relation.

742 If the input node and relation embeddings to the InGram model were to be the same across all nodes
743 and across all relation types respectively (such as vectors of all ones), then InGram would have
744 produced double structural representations for the triplets (definition 2.3). Simply put, this is because
745 the relation graphs proposed by Lee et al. (2023) [35] encode only the structural features of the
746 relation types (their mutual structural affinity), which is double equivariant to the permutation of
747 relation type and node indices. Since the same initial embeddings for all nodes and relations are
748 naively double equivariant, and the GATv2 [65, 6] is a message-passing neural network [27] that
749 also produces equivariant representations, the final relation embeddings would be double equivariant.
750 Same analysis will also show the final node embeddings are double equivariant.

751 However, to improve the expressivity of the model, Lee et al. (2023) [35] chose to randomly
752 re-initialize the input embeddings for all node and relation types using Glorot initialization [28]
753 for each epoch during training, a technique inspired by recent studies on the expressive power of
754 GNNs [1, 52, 42]. Unfortunately, random initial features break the double equivariance of the
755 generated representations, making them sensitive to the permutation of node and relation type indices.
756 However, since the initial node $\mathbf{V}^{(0)}$ and relation embeddings $\mathbf{R}^{(0)}$ are randomly initialized, and by

757 design of InGram architecture, we have $\forall(i, k, j) \in [N^{(*)}] \times [R^{(*)}] \times [N^{(*)}], \forall \phi \in \mathbb{S}_{N^{(*)}}, \tau \in$
758 $\mathbb{S}_{R^{(*)}}, \mathbf{Z}_{\text{InGram}}((i, k, j), \mathbf{A}^{(*)}, \mathbf{V}^{(0)}, \mathbf{R}^{(0)}) = \mathbf{Z}_{\text{InGram}}((\phi \circ i, \tau \circ k, \phi \circ j), \phi \circ \mathbf{A}^{(*)}, \mathbf{V}^{(0)}, \mathbf{R}^{(0)})$
759 for any random samples of node and relation embeddings $v^{(0)}, r^{(0)}$. We define $\mathbf{Z}_{\text{InGram}}|\mathbf{A}^{(*)} =$
760 $[\mathbf{Z}_{\text{InGram}}((i, k, j), \mathbf{A}^{(*)}, \mathbf{V}^{(0)}, \mathbf{R}^{(0)})]_{(i,k,j) \in [N^{(*)}] \times [R^{(*)}] \times [N^{(*)}]}$, and $\phi \circ \tau \circ \mathbf{Z}_{\text{InGram}}|\phi \circ \tau \circ \mathbf{A}^{(*)} =$
761 $[\mathbf{Z}_{\text{InGram}}((\phi \circ i, \tau \circ k, \phi \circ j), \phi \circ \tau \circ \mathbf{A}^{(*)}, \mathbf{V}^{(0)}, \mathbf{R}^{(0)})]_{(\phi \circ i, \tau \circ k, \phi \circ j) \in [N^{(*)}] \times [R^{(*)}] \times [N^{(*)}]}$. Since
762 $\mathbf{V}^{(0)}, \mathbf{R}^{(0)}$ random variables that do not change with permutations, we can easily derive $p(\phi \circ \tau \circ$
763 $\mathbf{Z}_{\text{InGram}}|\phi \circ \tau \circ \mathbf{A}^{(*)}) = p(\mathbf{Z}_{\text{InGram}}|\mathbf{A}^{(*)})$. Thus, InGram is a distributionally double equivariant
764 positional graph embedding of $\mathbf{A}^{(*)}$ as per Definition 2.7. \square

765 **Theorem B.2.** For any UQER Horn clause defined by $\mathbf{B} \in \{0, 1\}^{M \times K \times M}$ (Definition B.1),
766 there exists a double invariant triplet predictor $\Gamma_{\text{tri}} : \cup_{N=1}^{\infty} \cup_{R=2}^{\infty} ([N] \times [R] \times [N]) \times$
767 $\mathbb{A} \rightarrow \{0, 1\}$ (Definition 2.3), such that for any set of truth statements $\mathcal{S} \subseteq \mathcal{V}^{(*)} \times$
768 $\mathcal{R}^{(*)} \times \mathcal{V}^{(*)}$ and their equivalent tensor representation $\mathbf{A}^{(*)} \in \mathbb{A}$ (where $\mathbf{A}_{i,k,j}^{(*)} =$
769 1 iff $(v_i^{(*)}, r_k^{(*)}, v_j^{(*)}) \in \mathcal{S}$), it satisfies $\Gamma_{\text{tri}}((i, k, j), \mathbf{A}^{(*)}) = 1$ iff $(i, k, j) \in \mathcal{S}'$, where
770 $\mathcal{S}' = \{(i, k, j) \mid \forall(i, k, j), \text{ such that } (E_1, C_1, E_2) = (v_i^{(*)}, r_k^{(*)}, v_j^{(*)}) \in \mathcal{V}^{(*)} \times \mathcal{R}^{(*)} \times$
771 $\mathcal{V}^{(*)}, \exists^{M-2} E_3, \dots, E_M \in \mathcal{V}^{(*)} \setminus \{E_1, E_2\}, \exists^{K-1} C_2, \dots, C_K \in \mathcal{R}^{(*)} \setminus \{C_1\}, \text{ where } \forall(u, c, u') \in$
772 $[M] \times [K] \times [M], \mathbf{B}_{u,c,u'} = 1 \Rightarrow (E_u, C_c, E_{u'}) \in \mathcal{S}\}$ is the set of true statements induced by modus
773 ponens by the truth statements \mathcal{S} and the UQER Horn clause, where the existential quantifier \exists^k
774 means exists at least k distinct values.

775 *Proof.* Recall that we have two different cases $h = 1$ and $h = 2$ for Equation (5) in Definition B.1 of
776 UQER. For the ease of proof, we will focus on the case where $h = 2$ in the following content, and
777 for the case $h = 1$, the proof will be the same.

778 Given $h = 2$, any UQER is defined by $\mathbf{B} \in \{0, 1\}^{M \times K \times M}$ as

$$\forall E_1 \in \mathcal{V}^{(*)}, \left(\forall E_u \in \mathcal{V}^{(*)} \setminus \{E_1, \dots, E_{u-1}\} \right)_{u=2}^M, \forall C_1 \in \mathcal{R}^{(*)}, \left(\forall C_c \in \mathcal{R}^{(*)} \setminus \{C_1, \dots, C_{c-1}\} \right)_{c=2}^K, \\ \bigwedge_{\substack{u, u'=1, \dots, M, c=1, \dots, K, \\ \mathbf{B}_{u,c,u'}=1}} (E_u, C_c, E_{u'}) \implies (E_1, C_1, E_h), \quad (6)$$

779 for any node set $\mathcal{V}^{(*)}$ and relation set $\mathcal{R}^{(*)}$ with number of nodes and relations $N^{(*)}, R^{(*)}$ s.t.
780 $N^{(*)} \geq M, R^{(*)} \geq K$, where if $M > 2, \forall u \in \{3, \dots, M\}, \sum_{u'=1}^M \sum_{c=1}^K \mathbf{B}_{u,c,u'} + \mathbf{B}_{u',c,u} \geq 1$,
781 and if $K \geq 2, \forall c \in \{2, \dots, K\}, \sum_{u=1}^M \sum_{u'=1}^M \mathbf{B}_{u,c,u'} + \mathbf{B}_{u',c,u} \geq 1$ (every variable should appear
782 at least once in the formula).

783 For all sets of truth statements $\forall \mathcal{S} \subseteq \cup_{N=1}^{\infty} \cup_{R=2}^{\infty} \mathcal{V}^{(*)} \times \mathcal{R}^{(*)} \times \mathcal{V}^{(*)}$, it has an equivalent tensor
784 representation $\mathbf{A}^{(*)} \in \{0, 1\}^{N^{(*)} \times R^{(*)} \times N^{(*)}}$ such that $\mathbf{A}_{i,k,j}^{(*)} = 1 \iff (v_i^{(*)}, r_k^{(*)}, v_j^{(*)}) \in \mathcal{S}$. We
785 can then define a triplet representation Γ_{tri} based on the given UQER as, $\forall(i, k, j) \in [N^{(*)}] \times [R^{(*)}] \times$
786 $[N^{(*)}]$,

$$\Gamma_{\text{tri}}((i, k, j), \mathbf{A}^{(*)}) = \begin{cases} 1 & \text{if } (i, k, j) \in \mathcal{S}' \\ 0 & \text{otherwise,} \end{cases} \quad (7)$$

787 where we define $\mathcal{S}' = \{(i, k, j) \mid \forall(i, k, j) \in [N^{(*)}] \times [R^{(*)}] \times [N^{(*)}], \text{ such that } (E_1, C_1, E_2) =$
788 $(v_i^{(*)}, r_k^{(*)}, v_j^{(*)}) \in \mathcal{V}^{(*)} \times \mathcal{R}^{(*)} \times \mathcal{V}^{(*)}, \exists^{M-2} E_3, \dots, E_M \in \mathcal{V}^{(*)} \setminus \{E_1, E_2\}, \exists^{K-1} C_2, \dots, C_K \in$
789 $\mathcal{R}^{(*)} \setminus \{C_1\}, \text{ where } \forall(u, c, u') \in [M] \times [K] \times [M], \mathbf{B}_{u,c,u'} = 1 \Rightarrow (E_u, C_c, E_{u'}) \in \mathcal{S}\}$ is the set
790 of true statements induced by modus ponens from the truth statements \mathcal{S} and the UQER Horn Clause,
791 where the existential quantifier \exists^k means exists at least k distinct values.

792 All we need to show is that Equation (7) is a double invariant triplet representation. For any
793 node permutation $\phi \in \mathbb{S}_{N^{(*)}}$ and relation permutation $\tau \in \mathbb{S}_{R^{(*)}}$ of $\mathbf{A}^{(*)}$, we define $\phi \circ \tau \circ \mathcal{S} =$
794 $\{(v_{\phi \circ i}^{(*)}, r_{\tau \circ k}^{(*)}, v_{\phi \circ j}^{(*)}) \mid (v_i^{(*)}, r_k^{(*)}, v_j^{(*)}) \in \mathcal{S}\}$ which corresponds to their equivalent tensor represen-
795 tation $\phi \circ \tau \circ \mathbf{A}^{(*)}$, where $(\phi \circ \tau \circ \mathbf{A}^{(*)})_{\phi \circ i, \tau \circ k, \phi \circ j} = 1 \iff (v_i^{(*)}, r_k^{(*)}, v_j^{(*)}) \in \mathcal{S}$ other-
796 wise 0. Similarly, we have $\phi \circ \tau \circ \mathcal{S}' = \{(\phi \circ i, \tau \circ k, \phi \circ j) \mid \forall(i, k, j) \in [N^{(*)}] \times [R^{(*)}] \times$

797 $[N^{(*)}]$, such that $(E_1, C_1, E_2) = (v_{\phi \circ i}^{(*)}, r_{\tau \circ k}^{(*)}, v_{\phi \circ j}^{(*)}) \in \mathcal{V}^{(*)} \times \mathcal{R}^{(*)} \times \mathcal{V}^{(*)}$, $\exists^{M-2} E_3, \dots, E_M \in$
798 $\mathcal{V}^{(*)} \setminus \{E_1, E_2\}$, $\exists^{K-1} C_2, \dots, C_K \in \mathcal{R}^{(*)} \setminus \{C_1\}$, where $\forall(u, c, u') \in [M] \times [K] \times [M]$, $\mathbf{B}_{u,c,u'} =$
799 $1 \Rightarrow (\phi \circ E_u, \tau \circ C_c, \phi \circ E_{u'}) \in \phi \circ \tau \circ \mathcal{S}$.

By definition, we have that for any $(i, k, j) \in \mathcal{S}'$,

$$\Gamma_{\text{tri}}((\phi \circ i, \tau \circ k, \phi \circ j), \phi \circ \tau \circ \mathbf{A}^{(*)}) = \begin{cases} 1 & \text{if } (\phi \circ i, \tau \circ k, \phi \circ j) \in \phi \circ \tau \circ \mathcal{S}' \\ 0 & \text{otherwise,} \end{cases}$$

800 Now we show that $(i, k, j) \in \mathcal{S}'$ if and only if $(\phi \circ i, \tau \circ k, \phi \circ j) \in \phi \circ \tau \circ \mathcal{S}'$. If $(i, k, j) \in \mathcal{S}'$,
801 then $E_1 = v_i^{(*)}$, $E_2 = v_j^{(*)}$, $C_1 = r_k^{(*)}$, $\exists^{M-2} E_3, \dots, E_M \in \mathcal{V}^{(*)} \setminus \{E_1, E_2\}$, $\exists^{K-1} C_2, \dots, C_K \in$
802 $\mathcal{R}^{(*)} \setminus \{C_1\}$, such that $\mathbf{B}_{u,c,u'} = 1 \Rightarrow (E_u, C_c, E_{u'}) \in \mathcal{S}$. Since $(E_u, C_c, E_{u'}) \in \mathcal{S}$ if and only
803 if $(\phi \circ E_u, \tau \circ C_c, \phi \circ E_{u'}) \in \phi \circ \tau \circ \mathcal{S}$ by definition, we have $(\phi \circ i, \tau \circ k, \phi \circ j) \in \phi \circ \tau \circ \mathcal{S}'$.
804 Similarly we can prove if $(\phi \circ i, \tau \circ k, \phi \circ j) \in \phi \circ \tau \circ \mathcal{S}'$, then $(i, k, j) \in \mathcal{S}'$ with the same reasoning.

805 In conclusion, for any $\mathbf{A}^{(*)} \in \mathbb{A}$ with number of nodes and relations $N^{(*)}, R^{(*)}$, since $(i, k, j) \in \mathcal{S}'$
806 if and only if $(\phi \circ i, \tau \circ k, \phi \circ j) \in \phi \circ \tau \circ \mathcal{S}'$, then by definition $\Gamma_{\text{tri}}((\phi \circ i, \tau \circ k, \phi \circ j), \phi \circ \tau \circ \mathbf{A}^{(*)}) =$
807 $\Gamma_{\text{tri}}((i, k, j), \mathbf{A}^{(*)})$ holds $\forall(i, k, j) \in [N^{(*)}] \times [R^{(*)}] \times [N^{(*)}]$, which proves Γ_{tri} is a double invariant
808 triplet representation (Definition 2.3).

809 □

810 D Additional Related Work

811 Link prediction in discrete attributed multigraphs, which are commonly used to represent relational
812 data in a structured way by indicating different types of relations between pairs of nodes in the graph,
813 involves predicting not only the existence of missing edges but also the associated relation types.

814 **Transductive link prediction.** In transductive link prediction, missing links are predicted over a
815 fixed set of nodes and relation types as in training. Traditionally, factorization-based methods [59, 45,
816 5, 69, 76, 63, 44, 62, 19, 58] have been proposed to obtain latent embedding of nodes and relation
817 types to capture their relative information in the graph. These models try to score all combinations of
818 nodes and relations with embeddings as factors, similar to tensor factorization. Although excellence
819 in transductive tasks, these positional embeddings [54] (a.k.a. permutation-sensitive embeddings)
820 require extensive retraining to perform inductive tasks over new nodes or relations [60]. However, in
821 real-world applications, relational data is often evolving, requiring link prediction over new nodes
822 and new relation types, or even entirely new graphs.

823 **Inductive link prediction over new nodes (but not new relations) with GNN-based model.** In
824 recent years, with the advancement of graph neural networks (GNNs) [18, 33, 30, 64, 8, 43], in
825 graph machine learning fields, various works has applied the idea of GNN in relational prediction
826 to ensure the inductive capability of the model, including RGCN [53], GraIL [60], NodePiece [22],
827 NBFNet [87], ReFactorGNNs [14] etc.. As GNNs are node permutation equivariant [73, 54], these
828 models learn structural node/pairwise representation, which can be used to perform *inductive link*
829 *prediction over solely new nodes*, while most of the GNN performance are worse than FM-based
830 methods [50, 14]. Specifically, Teru et al. (2020) [60] extends the idea from [83] to use local
831 subgraph representations for discrete attributed multigraph link prediction. Chen et al. (2022b) [14]
832 aims to build the connection between FM and GNNs, where they propose an architecture to cast
833 FMs as GNNs. Galkin et al. (2021) [22] uses anchor-nodes for parameter-efficient architecture for
834 discrete attributed multigraph completion. Zhu et al. (2021) [87] extends the Bellman-Ford algorithm,
835 which learns pairwise representations by all the path representations between nodes. [2] analyzes
836 discrete attributed multigraph-GNNs expressiveness by connecting it with the Weisfeiler-Leman test
837 in discrete attributed multigraph.

838 **Inductive link prediction over new nodes (but not new relations) with logical induction.** The
839 relation prediction problem in relational data represented by discrete attributed multigraph can also
840 be considered as the problem of learning first-order logical Horn clauses [76, 77, 51, 60] from
841 the relational data, where one aims to extract logical rules on binary predicates. These methods

842 are inherently node-independent and are able to perform *inductive link prediction over solely new*
843 *nodes*. Barceló et al. (2020) [3] discusses the connection between the expressiveness of GNNs and
844 first-order logical induction, but only on node GNN representation and logical node classifier. Qiu
845 et al. (2023) [47] further analyzes the logical expressiveness of GNNs for attributed multigraph by
846 showing GNNs are able to capture logical rules from graded modal logic and provides a logical
847 explanation of why pairwise GNNs [84, 87] can achieve SOTA results. In our paper, we try to build
848 the connection between triplet representation and logical Horn clauses. Traditionally, logical rules are
849 learned through statistically enumerating patterns observed in discrete attributed multigraph [34, 21].
850 Neural LP [77] and DRUM [51] learn logical rules in an end-to-end differentiable manner using
851 the set of logic paths between two nodes with sequence models. Cheng et al. (2022) [15] follows a
852 similar manner, which breaks a big sequential model into small atomic models in a recursive way.
853 Galkin et al. (2022) [23] aims to inductively extract logical rules by devising NodePiece [22] and
854 NBFNet [87]. However, all these methods are not able to deal with new relation types in test.

855 **Inductive link prediction over both new nodes and new relations (with extra context)** Few-shot
856 and zero-shot relational reasoning [72, 38, 46, 85, 24, 67, 31, 11, 25] aim to query triplets involving
857 unseen relation types with access to few or zero support triplets of these unseen relation types at
858 test time. Recent methods [46, 85, 31, 25] can even query over unseen nodes. Yet, they often need
859 extra context in the test graph, such as textual descriptions and/or ontological information of the
860 unseen relation types or a shared background graph between the training and test graph, i.e., the test
861 nodes and relation types are connected to the training ones. For instance, zero-shot link prediction
862 methods such as Qin et al. (2020) [46] employ a generative adversarial network [29] to utilize
863 the additional textual information to bridge the semantic gap between seen and unseen relations.
864 Later, Geng et al. (2021) [24] presented an ontology-enhanced zero-shot learning approach that
865 incorporates both ontology structural and textural information. Similarly, TACT [10] aims to model
866 the topological correlations between the target relations and their adjacent relations (assumes there
867 are relations that are seen in train) using a relational correlation network to learn more expressive
868 representations of the target relations. A recent work is RMPI [25] that extracts enclosing subgraphs
869 around the target triplet, which are assumed to contain triplets of some relation types seen in training
870 and uses graph ontology to bridge the unseen relation types to the seen ones. Zhao et al. (2020) [85]
871 uses attention-based GNNs and convolutional transition for link prediction over new nodes and new
872 relations assuming a shared background graph between training and test (i.e., new relations in test
873 are connected with existing nodes and relations in training). MaKER [12] also uses the local graph
874 structure to handle new nodes and new relation types using a meta-learning framework, assuming
875 the test graph has overlapping relations and entities with the training graph. On the other hand,
876 few-shot relational reasoning methods learn representations of the unseen relation types from the
877 few support triplets, which are generally assumed to connect to existing nodes and relations seen in
878 training [72, 13, 82]. For example, Xiong et al. (2018) [72] was the first to solve the one-shot task by
879 proposing to compute matching scores between the new relation types observed in the support set to
880 those training relation types. Later, Zhang et al. (2020) [82] extends Xiong et al. (2018) [72] by using
881 an attention-based aggregation to take advantage of information from all support triplets. Recently,
882 Huang et al. (2020) [31] proposed a hypothesis testing method that matches the new relation types to
883 the training ones by learning to compare the similarity between the connection subgraph patterns
884 surrounding the target triplets. Another line of research is to solve few-shot relational reasoning via
885 meta-learning. For instance, Chen et al. (2019) [13] updates a meta representation over the relation
886 types, and Lv et al. (2019) [38] adopts MAML [20] to learn meta parameters for frequently occurring
887 relations, which can then be adapted to few-shot relations. All of these few-shot learning methods,
888 however, require that the few-shot triplets are connected to a background graph observed during
889 training in order to learn about the relationship between new relation types and existing ones. Hence,
890 all these methods cannot be directly applied to test graphs that neither contain textual descriptions of
891 the unseen relation types nor triplets involving those relation types seen in training.

892 **Inductive link prediction over both new nodes and new relations (no extra context)** In this
893 paper, we focus on the most general task, i.e., inductive link prediction over both new nodes and new
894 relations on entirely new test graphs without textual descriptions, which we call *doubly inductive link*
895 *prediction*. To the best of our knowledge, InGram [35] is the first and only existing method capable
896 of performing this task. In contrast to Lee et al. (2023) [35] that designed a specific architecture, i.e.,
897 InGram, our work proposes a general theoretical framework for designing an entire class of models

898 capable of solving the doubly inductive link prediction task, which encompasses InGram as a specific
899 instantiation. Modeling details of InGram have been substantially discussed in the main paper.

900 **Knowledge graph alignment.** Knowledge graph alignment tasks [55, 56, 75, 57] are very common
901 in heterogeneous, cross-lingual, and domain-specific relational data, where the task aims to align
902 nodes among different domains. For example, matching nodes with their counterparts in different
903 languages [70, 74]. It is intrinsically different than our task, where we aim to inductively apply on
904 completely new nodes and relations, possibly with no clear alignments between them.

905 E Experiments

906 Our code is available at <https://anonymous.4open.science/r/ISDEA-Fix-B3D7>.

907 E.1 Doubly inductive link prediction task over both new nodes and new relation types

908 In this section, we provide more detailed experiment results and analysis for our method on inductively
909 doubly inductive link prediction on both new nodes and new relation types.

910 **Datasets.** To the best of our knowledge, there are no existing real-world benchmarks that are specially
911 designed to test a model’s extrapolation capability for doubly inductive link prediction task by training
912 the model on one graph and testing it on another completely new graph coming from different domains
913 and distributions. Existing datasets such as NL-100, WK-100, and FB-100 from Lee et al. (2023) [35]
914 are typically created by randomly splitting a larger graph (e.g. NELL-995 [72], Wikidata68K [26],
915 FB15K237 [61]) into disjoint node and relation sets, implying that the test and training graphs still
916 come from the same distribution. In contrast, we purposefully create two doubly inductive link
917 prediction benchmark datasets: PediaTypes and WikiTopics, sampled respectively from the OpenEA
918 library [57] and WikiData-5M [68], where by design the test and training graphs are either from
919 different domains or different topic groups and are likely to possess different characteristics to fully
920 test model’s capability for doubly inductive link prediction. We also propose another task with
921 modifications of the NL- k , WK- k , and FB- k datasets from InGram [35] and one synthetic task FD2
922 to study the expressive power of ISDEA.

923 E.1.1 Experiment Setup

924 **Baselines.** To the best of our knowledge, InGram [35] is the first and only work capable of
925 performing doubly inductive link prediction without needing significant modification to the model.
926 Hence, we chose InGram as one baseline. We also run RMPI [25], which is capable of reasoning
927 over new nodes and new relations but requires extra context at test time (test graphs either contain
928 training relations or ontological information of unseen relations). We simply provide randomized
929 embeddings of unseen relations at test time following Lee et al. (2023) [35]. In addition, we consider
930 the state-of-the-art link prediction model NBFNet [87] capable of generalizing over to new nodes but
931 not new relations and modifying its architecture to work with new relations at test time by providing
932 randomized embeddings of unseen relations at test time following Lee et al. (2023) [35]. We also
933 compare our models with message-passing GNNs including GAT [64], GIN [73], GraphConv [41]
934 which treats the graph as a homogeneous graph by ignoring the relation types. For fair comparisons,
935 we add distance features as in Equation (2) to increase the expressiveness of these GNNs. For training
936 of each single run, we augment each triplet (i, k, j) by its inversion (i, k^{-1}, j) , and sample 2 negative
937 (node) triplets (i', k, j') and 2 negative (relation) triplets (i, k', j) per positive in training as Sun et
938 al. (2018) [58] and Zhu et al. (2021) [87]. Training was performed on NVidia A100s, L4s, GeForce
939 RTX 2080 Ti, and TITAN V GPUs.

940 **Evaluation Metrics.** We sample 50 negative triplets for each test positive triplet during test
941 evaluation by corrupting either nodes or relation types (Equation (3)), and use Nodes Hits@ k and
942 Relation Hits@ k separately which counts the ratio of positive triplets ranked at or above the k -th
943 place against the 50 negative samples as evaluation metric over 5 runs. Specifically, for Node
944 prediction evaluation, we sample without replacement 50 negative tail (or head) nodes, and for
945 Relation prediction evaluation, we sample with replacement 50 negative relation types (can also
946 handle cases where the number of test relations is less than 50). We also report other widely used
947 metrics such as MRR.

948 **Hyperparameters and Implementation Details.** For homogeneous GNN methods, NBFNet and
949 ISDEA, We follow the same configuration as Teru et al. (2020) [60] such that the hidden layers have
950 32 neurons. We use Adam optimizer with grid search over learning rate $\alpha \in \{0.01, 0.001, 0.0001\}$,
951 and over weight decay $\beta \in \{0.0005, 0\}$. For all datasets, we train these models for 10 epochs with a
952 mini-batch size of 16. For the GNN kernel (e.g., GraphConv, GIN, GAT) of ISDEA, we choose the
953 best-performing model in validation. For these models, the number of hops and number of layers are
954 2 on FD-2, and 3 on all other datasets to ensure fair comparison.

955 Since NBFNet is designed to only perform inductive link prediction with solely new nodes and
956 utilizes trained relation embeddings, we use randomly initialized embeddings for the unseen relation
957 types at test time to enable it for performing doubly inductive link prediction.

958 To run InGram [35] on PediaTypes and WikiTopics, we conduct hyperparameter search over the
959 configurations of ranking loss margin $\gamma \in \{1.0, 2.0\}$, learning rate $\alpha \in \{0.0005, 0.001\}$, number of
960 entity layers $L \in \{2, 3, 4\}$, and number of entity layers $\hat{L} \in \{2, 3, 4\}$. For other hyperparameters,
961 we use the suggested values from Lee et al. (2023) [35] and their codebase, such as the number of
962 bins $B = 10$ and the number of attention heads $K = 8$. We then use the overall best-performing
963 hyperparameters on PediaTypes and the best-performing hyperparameters on WikiTopics to run
964 InGram on all tasks in PediaTypes and all tasks in WikiTopics respectively. For running on the
965 (modified) NL- k , WK- k , and FB- k datasets from Lee et al. (2023) [35], we use the provided
966 hyperparameters for each task from the authors.

967 To run DEq-InGram, we use the same trained checkpoints of InGram. The difference is at inference
968 time, where instead of a single forward pass with one sample of randomly initialized entity and
969 relation embeddings for InGram, we draw 10 samples of initial entity and relation embeddings and
970 run 10 forward passes. This yields 10 Monte Carlo samples of the triplet scores, which we then use
971 to compute the DEq-InGram triplet scores according to Equation (4).

972 For RMPI [25], we use the provided hyperparameters from the codebase and run the RMPI-NE
973 version of the model with a concatenation-based fusion function, which generally has the best
974 performance reported in Geng et al. (2023) [25]. We note that, since our attributed multigraph does
975 not contain ontological information over the unseen relation types of the test graphs, we instead
976 provide the model with randomly initialized embeddings for the unseen relation types to perform
977 doubly inductive link prediction.

978 E.1.2 Doubly inductive link prediction over PediaTypes

979 As discussed in Section 5, we create our own doubly inductive link prediction benchmark dataset
980 PediaTypes. Each graph in PediaTypes is sampled from a graph in the OpenEA library [57] (under
981 GPL-3.0 license). OpenEA [57] library provides multiple pairs of attributed multigraph, each pair
982 of which is a database containing similar topics. Each node of a graph corresponds to the Universal
983 Resource Identifier (URI) of an entity in the database, e.g., “<http://dbpedia.org/resource/E399772>”
984 from English DBPedia. Each relation type of a graph corresponds to the URI of a relation in
985 the database, e.g., “<http://dbpedia.org/ontology/award>” from English DBPedia. Moreover, since
986 each pair of graphs describes similar topics, most entities and relations are highly related, e.g.,
987 “<http://dbpedia.org/resource/E678522>” from English and “<http://fr.dbpedia.org/resource/E415873>”
988 from French are indeed the same thing, except that the labeling is different. Thus, we would expect a
989 powerful model that is insensitive to node and relation type labelings to be able to learn on one graph
990 of the pair and perform well on the other graph of the same pair.

991 To control the size under a feasible limitation, we use the same subgraph sampling algorithm as
992 GraIL [60], which proposes link prediction benchmarks over solely new nodes. Details are provided
993 in Algorithm 1. For each pair of graphs from the OpenEA library, e.g., English-to-French DBPedia,
994 we first apply the sampling algorithm as in Algorithm 1 on each graph to reduce the size of each
995 graph. Then we randomly split querying triplets given by the Algorithm 1 into 80% training, 10%
996 validation, and 10% test for each graph. Finally, to construct the task where we learn on English
997 DBPedia but test on French DBPedia (denoted as EN-FR), we pick training and validation triplets
998 from the English graph for model tuning, and only use test triplets from the French graph for model
999 evaluation; Similarly, for task from French to English (FR-EN), we pick training and validation
1000 triplets from French graph for model tuning, and only use test triplets from English graph for model
1001 evaluation. The **dataset statistics** for PediaTypes are summarized in Figure 6.

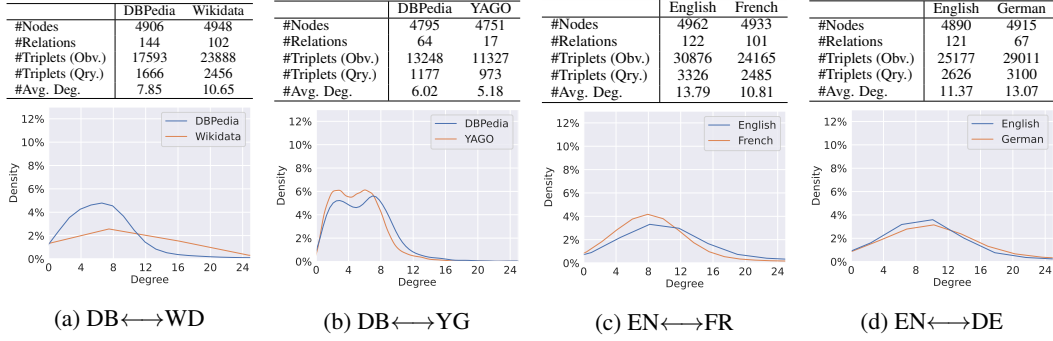


Figure 6: **Statistics of PediaTypes:** We report graph statistics including the number of nodes, number of relations, observed (obv.) triplets, querying (qry.) triplets, and average degree for each graph pair, e.g., (a) corresponds to DBPedia-and-Wikidata pair, and will be used to construct DB2WD and WD2DB tasks. We also report (in & out) degree distribution on each graph at the bottom. We omit tail distribution larger than 25 since they are too small and almost flat.

Algorithm 1 Sampling Algorithm for PediaTypes. This is a subgraph sampling code for a single graph (either training or test). It will reduce the large original graph into a connected graph of the required size.

Require: Raw graph triplets \mathcal{S}^{raw} , Raw graph node set \mathcal{V}^{raw} , Raw graph relation set \mathcal{R}^{raw} , Maximum number of nodes N , Maximum number of edges M , Maximum node degree D .

Ensure: Subgraph triplets \mathcal{S}^{sub}

```

1:  $\mathcal{S}^{\text{sub}} \leftarrow \emptyset$ 
2:  $\mathcal{V}^{\text{sub}} \leftarrow \emptyset$ 
3:  $\mathcal{R}^{\text{sub}} \leftarrow \emptyset$ 
4: Create an empty queue  $Q$ .
5: Get the node  $v_0$  with the highest degree in the raw graph.
6:  $Q.add(v_0)$ 
7:  $\mathcal{V}^{\text{sub}} \leftarrow \mathcal{V}^{\text{sub}} \cup \{v_0\}$ 
8: while  $|Q| > 0$  do
9:    $u \leftarrow Q.pop()$ 
10:  if  $|\mathcal{V}^{\text{sub}}| \geq N$  or  $|\mathcal{E}^{\text{sub}}| \geq M$  then
11:    continue
12:  end if
13:   $\mathcal{B} = \{(v, r, u) | (r, v) \in \mathcal{R}^{\text{raw}} \times \mathcal{V}^{\text{raw}}\} \cup \{(u, r, v) | (r, v) \in \mathcal{R}^{\text{raw}} \times \mathcal{V}^{\text{raw}}\}$ 
14:  if  $|\mathcal{B}| > D$  then
15:    Uniformly select  $D$  triplets from  $\mathcal{B}$  as  $\mathcal{B}'$ 
16:  else
17:     $\mathcal{B}' \leftarrow \mathcal{B}$ 
18:  end if
19:  for  $(i, r, j) \in \mathcal{B}'$  do
20:    if  $i = u$  then
21:       $Q.add(j)$ 
22:       $\mathcal{V}^{\text{sub}} \leftarrow \mathcal{V}^{\text{sub}} \cup \{j\}$ 
23:    else
24:       $Q.add(i)$ 
25:       $\mathcal{V}^{\text{sub}} \leftarrow \mathcal{V}^{\text{sub}} \cup \{i\}$ 
26:    end if
27:     $\mathcal{S}^{\text{sub}} \leftarrow \mathcal{S}^{\text{sub}} \cup \{(i, r, j)\}$ 
28:  end for
29: end while

```

Table 2: **Relation & Node MRR performance on Doubly Inductive Link Prediction over PediatrTypes**. We report standard deviations over 5 runs. A higher value means better doubly inductive link prediction performance. “Rand” column contains unbiased estimations of the performance from a random predictor. **Both ISDEA and DEq-InGram consistently achieve better results than the baselines**. N/A*: Not available due to constant crashes.

(a) Relation prediction ($i, j, ?$) performance in %. Higher \uparrow is better.

Models	EN-FR	FR-EN	EN-DE	DE-EN	DB-WD	WD-DB	DB-YG	YG-DB
Rand	8.86±00.00	8.86±00.00	8.86±00.00	8.86±00.00	8.86±00.00	8.86±00.00	8.86±00.00	8.86±00.00
GAT	8.04±00.25	7.93±00.04	8.17±00.08	8.12±00.09	8.06±00.15	7.90±00.12	8.12±00.21	8.17±00.16
GIN	8.07±00.09	8.09±00.05	8.07±00.13	8.07±00.11	8.03±00.20	7.97±00.30	7.82±00.27	7.84±00.14
GraphConv	7.92±00.16	7.97±00.12	8.07±00.15	8.03±00.05	8.14±00.04	7.98±00.18	8.04±00.24	7.84±00.13
NBFNet	10.25±01.24	9.53±00.85	8.15±01.21	4.32±00.26	10.33±02.45	8.97±01.24	9.29±01.38	14.54±04.76
RMPI	12.45±01.90	12.10±02.71	11.69±04.37	10.28±01.28	N/A*	8.54±02.70	17.89±12.22	6.53±02.16
InGram	50.03±05.32	26.31±08.27	21.32±07.84	29.81±14.21	48.70±10.06	38.81±03.10	29.94±13.28	32.26±13.97
DEq-InGram (Ours)	73.38 ±05.77	41.61 ±10.12	46.86 ±09.11	40.56 ±14.80	80.74 ±04.47	66.06 ±02.91	39.51 ±16.76	49.10 ±05.43
ISDEA (Ours)	<u>70.06</u> ±02.01	69.01 ±00.57	78.38 ±04.04	88.82 ±00.28	<u>65.89</u> ±04.71	72.57 ±00.73	75.88 ±01.58	74.04 ±00.47

(b) Node prediction ($i, k, ?$) performance in %. Higher \uparrow is better.

Models	EN-FR	FR-EN	EN-DE	DE-EN	DB-WD	WD-DB	DB-YG	YG-DB
Rand	8.86±00.00	8.86±00.00	8.86±00.00	8.86±00.00	8.86±00.00	8.86±00.00	8.86±00.00	8.86±00.00
GAT	51.43±00.25	49.48±01.51	26.22±00.44	25.45±01.23	16.87±00.59	34.66±00.33	37.22±00.29	45.96±00.29
GIN	53.72±03.45	52.03±03.38	34.60±07.43	37.27±09.42	20.75±07.22	40.37±08.20	35.80±01.36	44.77±00.92
GraphConv	63.72±01.76	57.77±01.09	48.18±00.96	45.18±00.15	22.49±00.76	50.30±02.80	38.71±00.55	50.54±00.42
NBFNet	<u>69.22</u> ±02.44	74.01 ±01.41	63.49 ±02.44	38.86±02.55	41.26±02.58	64.02 ±01.25	38.13±01.11	52.30±02.09
RMPI	63.02±02.94	43.72±05.65	44.82±02.93	46.84±05.36	N/A*	46.33±08.76	43.00 ±03.70	53.72 ±01.84
InGram	71.23±01.73	55.67±05.65	55.94±02.76	<u>61.15</u> ±01.42	34.50±08.47	57.05±03.73	26.36±04.73	56.23 ±01.56
DEq-InGram (Ours)	78.45 ±00.89	68.59 ±04.30	66.13 ±01.48	70.32 ±01.58	<u>44.71</u> ±08.98	69.23 ±02.53	35.67±03.92	48.07±08.76
ISDEA (Ours)	53.92±00.26	57.68±00.68	50.30±02.08	51.33±00.40	45.75 ±00.66	51.64±00.60	<u>41.72</u> ±01.64	48.21±01.06

1002 **Additional Results** We present the Node & Relation Hits@10 performance in the main paper.
1003 We provide more results including MRR, Hits@1, Hits@5 in Tables 2 to 4. We can see that our
1004 proposed ISDEA and DEq-InGram perform consistently and significantly better than the baselines in
1005 the much harder relation prediction task, showing their power to generalize to both new nodes and
1006 new relations. The structural double equivariant model ISDEA performs worse on node prediction
1007 over some datasets, which might be due to the node GNN implementation of ISDEA. These tasks
1008 do not care much about the actual relation type as we can see from the superior performance of
1009 homogeneous GNNs on node prediction. So the additional equivariance over relations and the
1010 training loss over both negative nodes and negative relations might cause the model to focus more
1011 on the relation prediction task, while the double equivariant structural representation might hurt the
1012 performance of missing node prediction [54].

1013 But it is important to note that the structural double equivariant ISDEA model excels on relation
1014 prediction and achieves much better results on Hits@1 and Hits@5 as shown in Tables 3 and 4.
1015 The performance of baseline models that is lower than random is probably because the knowledge
1016 they learn from one dataset is not able to correctly transform to another dataset, while our double
1017 equivariant model architecture is able to perform this hard doubly inductive link prediction over both
1018 new nodes and new relation types. We also note that in the Hits@1 and Hits@5 Tables 3 and 4, there
1019 are cases where DEq-InGram has higher variances than the original InGram while achieving much
1020 better average performance. This is because due to the random initialization, InGram performs poorly
1021 on the much harder Hits@1 and Hits@5 performance compared to Hits@10. In some seeds of the
1022 runs, DEq-InGram successfully improves the performance of InGram, but there are still seeds of runs
1023 that DEq-InGram still performs similar to InGram. Thus, it results in DEq-InGram having much
1024 better average results while also with higher standard deviations.

1025 E.1.3 Doubly inductive link prediction over WikiTopics

1026 As discussed in Section 5.2, the WikiTopics dataset is created from the WikiData-5M [68] (under
1027 CC0 1.0 license). Each node in the graphs of this dataset represents an entity described by an existing
1028 Wikipedia page, and each relation type corresponds to a particular relation between the entities,
1029 such as “director of” or “designed by”. The node and relation type indices are codenames that start

Table 3: **Relation & Node Hits@1 performance on Doubly Inductive Link Prediction over PediaTypes.** We report standard deviations over 5 runs. A higher value means better doubly inductive link prediction performance. “Rand” column contains unbiased estimations of the performance from a random predictor. **Both ISDEA and DEq-InGram consistently achieve better results than the baselines.** N/A*: Not available due to constant crashes.

(a) Relation prediction ($i, ?, j$) performance in %. Higher \uparrow is better.

Models	EN-FR	FR-EN	EN-DE	DE-EN	DB-WD	WD-DB	DB-YG	YG-DB
Rand	1.96±00.00	1.96±00.00	1.96±00.00	1.96±00.00	1.96±00.00	1.96±00.00	1.96±00.00	1.96±00.00
GAT	1.07±00.14	1.01±00.01	1.03±00.03	1.11±00.09	1.07±00.14	0.99±00.21	0.96±00.16	1.09±00.25
GIN	1.01±00.03	0.95±00.08	1.03±00.06	1.10±00.06	0.96±00.15	1.00±00.15	0.92±00.15	0.83±00.17
GraphConv	0.91±00.03	0.97±00.06	1.05±00.14	1.01±00.03	1.09±00.07	0.91±00.04	0.94±00.22	0.88±00.20
NBFNet	4.43±01.24	3.62±01.01	2.49±01.23	0.51±00.18	4.18±02.17	2.80±00.83	1.63±00.89	7.30±05.01
RMPI	3.92±02.08	4.04±01.83	3.37±02.20	2.13±00.79	N/A*	2.39±02.35	7.36±09.03	0.91±00.92
InGram	35.19±07.73	12.40±07.55	8.45±06.57	16.46±16.33	33.66±12.09	25.69±03.88	14.24±12.00	15.83±12.59
DEq-InGram (Ours)	65.26 ±10.23	26.90 ±12.97	36.80 ±11.16	25.34 ±18.48	75.00 ±06.42	60.35 ±02.56	24.28 ±14.29	30.82 ±10.43
ISDEA (Ours)	61.46 ±00.79	58.18 ±00.14	68.00 ±06.41	84.83 ±00.29	57.51 ±05.40	62.72 ±01.24	69.12 ±02.40	66.68 ±00.81

(b) Node prediction ($i, k, ?$) performance in %. Higher \uparrow is better.

Models	EN-FR	FR-EN	EN-DE	DE-EN	DB-WD	WD-DB	DB-YG	YG-DB
Rand	1.96±00.00	1.96±00.00	1.96±00.00	1.96±00.00	1.96±00.00	1.96±00.00	1.96±00.00	1.96±00.00
GAT	31.80±00.64	30.19±02.30	10.23±00.96	8.68±01.69	7.98±00.89	16.26±00.34	26.09±00.47	33.06±00.29
GIN	34.59±04.64	34.57±05.26	17.69±07.91	20.74±10.01	12.42±06.59	23.10±09.67	23.72±01.62	32.26±01.89
GraphConv	47.48±02.60	40.37±01.52	31.96±01.02	28.46±00.13	12.53±00.34	35.82±03.54	24.12±00.80	37.05±00.51
NBFNet	64.17 ±02.68	69.68 ±01.63	57.50 ±02.66	32.26±02.81	34.56 ±02.54	59.70 ±01.38	33.32 ±01.11	47.47 ±02.08
RMPI	48.27±03.74	26.92±04.87	27.38±03.09	29.60±04.77	N/A*	34.81±08.97	33.29 ±03.20	42.14 ±02.87
InGram	60.00±02.06	41.59±06.37	39.05±02.99	45.44 ±01.69	22.06±08.10	42.54±04.50	13.47±03.50	20.09±04.96
DEq-InGram (Ours)	69.46 ±01.12	57.65 ±05.54	51.93 ±01.88	57.06 ±01.96	32.12±09.51	57.84 ±03.28	20.49±03.35	33.01±08.87
ISDEA (Ours)	43.03±00.25	47.38±00.28	35.41±02.25	37.12±00.31	35.59 ±00.73	40.56±01.72	27.70±01.95	35.29±01.67

1030 with the prefix “Q” and “P” respectively, which are devoid of semantic meaning. Nevertheless,
 1031 WikiData-5M [68] provides aliases for all nodes and relation types that map their indices to textual
 1032 descriptions, and we use these textual descriptions to group the relation types into 11 different topics
 1033 (we do not however provide these textual descriptions to the models per the specification of the
 1034 doubly inductive link prediction task). In total, WikiData-5M [68] contains 822 relation types. We
 1035 create WikiTopics datasets from all 822 relation types, which comprise graphs with as many as 66
 1036 relation types. Each graph has a disjoint set of relation types from all other graphs. Below is a list of
 1037 all 11 topics:

- 1038 • T1: Art and Media Representation
- 1039 • T2: Award Nomination and Achievement
- 1040 • T3: Education and Academia
- 1041 • T4: Health, Medicine, and Genetics
- 1042 • T5: Infrastructure and Transportation
- 1043 • T6: Location and Administrative Entity
- 1044 • T7: Organization and Membership
- 1045 • T8: People and Social Relationship
- 1046 • T9: Science, Technology, and Language,
- 1047 • T10: Sport, and Game Competition
- 1048 • T11: Taxonomy and Biology

1049 To control the overall size of the graphs in WikiTopics, we downsample 10,000 nodes for each topic
 1050 from the subgraph consisting of only the triplets with the relation types belonging to that topic. We
 1051 adopt the Forest Fire sampling procedure with burning probability $p = 0.8$ [37] implemented in
 1052 the Little Ball of Fur Python package [49]. We then split the downsampled topic graph into 90%
 1053 observable triplets and 10% querying triplets to be predicted by the models. When splitting, we
 1054 ensure that the set of nodes in the querying triplets is a subset of those in the observable triplets. This

Table 4: **Relation & Node Hits@5 performance on Doubly Inductive Link Prediction over PediaTypes.** We report standard deviations over 5 runs. A higher value means better doubly inductive link prediction performance. “Rand” column contains unbiased estimations of the performance from a random predictor. **Both ISDEA and DEq-InGram consistently achieve better results than the baselines.** N/A*: Not available due to constant crashes.

(a) Relation prediction ($i, ?, j$) performance in %. Higher \uparrow is better.

Models	EN-FR	FR-EN	EN-DE	DE-EN	DB-WD	WD-DB	DB-YG	YG-DB
Rand	9.80±00.00	9.80±00.00	9.80±00.00	9.80±00.00	9.80±00.00	9.80±00.00	9.80±00.00	9.80±00.00
GAT	9.08±00.39	8.63±00.25	9.47±00.18	9.20±00.24	8.95±00.36	8.63±00.29	9.58±00.50	9.16±00.23
GIN	9.09±00.16	9.31±00.15	9.18±00.28	9.23±00.34	9.12±00.12	8.85±00.56	8.53±00.66	8.61±00.34
GraphConv	8.97±00.66	8.74±00.26	9.23±00.11	8.82±00.10	9.17±00.29	9.11±00.50	9.01±00.72	8.73±00.15
NBFNet	12.94±01.77	12.46±01.40	8.56±01.67	2.68±00.72	13.44±04.02	11.74±03.02	11.95±03.78	20.37±05.90
RMPI	16.39±04.15	15.76±04.58	15.86±08.05	12.56±02.70	N/A*	8.91±03.51	24.25±19.24	4.98±03.08
InGram	67.15±05.04	37.86±14.41	30.99±11.82	40.00±13.02	65.80±09.59	51.66±03.57	43.27±19.30	51.54±26.09
DEq-InGram (Ours)	83.23 ±05.64	<u>59.83</u> ±11.57	<u>54.30</u> ±08.25	<u>57.65</u> ±15.74	87.08 ±02.55	<u>70.79</u> ±03.80	<u>51.45</u> ±29.14	<u>75.85</u> ±07.26
ISDEA (Ours)	<u>82.11</u> ±04.01	83.19 ±01.73	92.39 ±00.83	93.59 ±00.53	<u>75.95</u> ±03.89	86.10 ±01.26	85.80 ±01.23	83.36 ±01.55

(b) Node prediction ($i, k, ?$) performance in %. Higher \uparrow is better.

Models	EN-FR	FR-EN	EN-DE	DE-EN	DB-WD	WD-DB	DB-YG	YG-DB
Rand	9.80±00.00	9.80±00.00	9.80±00.00	9.80±00.00	9.80±00.00	9.80±00.00	9.80±00.00	9.80±00.00
GAT	78.49±00.44	74.70±00.68	42.17±00.91	42.39±00.52	20.96±00.65	57.26±00.89	46.92±00.37	59.20±00.41
GIN	79.96±01.88	74.33±01.16	53.97±07.61	55.89±10.06	25.05±09.23	61.94±06.71	46.56±01.37	57.48±00.35
GraphConv	85.21±00.63	80.67±00.30	67.76±01.19	64.97±00.43	28.37±01.41	67.36±02.37	53.79±00.72	64.13±00.23
NBFNet	81.48±02.24	85.15 ±01.06	77.62±02.41	48.73±02.59	51.52±03.21	<u>72.18</u> ±00.90	44.01±01.40	60.34±02.28
RMPI	82.47±02.25	64.88±07.62	67.24±04.38	69.47±06.60	N/A*	60.11±08.77	51.57±05.03	66.67 ±01.28
InGram	<u>85.15</u> ±01.74	72.32±05.31	<u>78.84</u> ±02.86	<u>81.01</u> ±00.97	45.96±11.09	74.88±03.09	37.49±06.84	50.66±06.76
DEq-InGram (Ours)	89.62 ±00.63	<u>81.54</u> ±02.82	84.57 ±00.95	87.16 ±01.04	57.44 ±09.14	83.14 ±01.64	51.77±05.14	<u>65.33</u> ±09.57
ISDEA (Ours)	64.45±00.24	67.24±01.32	68.80±01.90	68.20±00.53	<u>54.83</u> ±00.90	62.60±02.55	55.21 ±01.07	61.87±01.30

1055 way, the model is not tasked with the impossible task of predicting relation types between orphaned
1056 nodes previously unseen in the observable part of the graph. This is implemented via an iterative
1057 procedure, where we first sample a batch of missing triplets from the downsampled topic graph,
1058 then discard those that contain unseen nodes in the rest of the triplets, and repeat this process until
1059 the number of sampled triplets reaches 10% of total triplets. Figure 7 shows the **data statistics** of
1060 WikiTopics dataset.

1061 **Additional experiment results on WikiTopics.** In Section 5.2, we only provide heatmaps of
1062 Relation Hits@10 Performance WikiTopics due to space limit. We present more detailed results
1063 (heatmaps with values) of Node and Relation Hits@10, Hits@1, and MRR for WikiTopics in Figures 8
1064 and 9. Due to the large number of runs ($11 \times 10 = 110$ different train-test scenarios, each with 5
1065 random seeds, resulting in a total of 550 runs) and the time constraints to run all baseline models,
1066 we perform the evaluation over only the three models (ISDEA, DEq-InGram, and InGram) that are
1067 designed for our doubly inductive link prediction task. Figure 8 shows that for the task of predicting
1068 missing relation types ($i, ?, j$), ISDEA and DEq-InGram are consistently better than InGram across
1069 all different metrics. Especially, the structural double equivariant ISDEA model exhibits more
1070 consistent results across different train-test scenarios than both DEq-InGram and InGram, and
1071 achieves significantly better results in Hits@1 and MRR, showcasing its ability for doubly inductive
1072 link prediction in a much harder evaluation scenario. For the task of prediction missing nodes ($i, k, ?$)
1073 as shown in Figure 9, ISDEA, DEq-InGram, and InGram showcase comparable performance, whereas
1074 ISDEA exhibits more consistent results across different train-test scenarios than both DEq-InGram
1075 and InGram. We also note that similar to the relation prediction task, ISDEA also exhibits the best
1076 performance in the Hits@1 metric for the node prediction task.

1077 **E.1.4 Doubly Inductive Link Prediction over datasets from InGram (Lee et al., 2023)**

1078 Lee et al. (2023) [35] proposed the NL- k , WK- k , and FB- k benchmarks originally used to evaluate
1079 InGram’s performance of reasoning over new nodes and new relation types at test time, where
1080 $k \in \{25, 50, 75, 100\}$ means that, in the test graphs, approximately $k\%$ of triplets have unseen
1081 relations. For example, the test graph of WK-100 does not contain any training relations and thus
1082 induces a doubly inductive link prediction task. Hence, we run our models (ISDEA and DEq-InGram)

	#Nodes	# Relations	#Triplets (Obv.)	#Triplets (Qry.)	Avg. Deg.
Art	10000	45	28023	3113	6.23
Award	10000	10	25056	2783	5.57
Education	10000	15	14193	1575	3.15
Health	10000	20	15337	1703	3.41
Infrastructure	10000	27	21646	2405	4.81
Location	10000	35	80269	8918	17.84
Organization	10000	18	30214	3357	6.71
People	10000	25	58530	6503	13.01
Science	10000	42	12516	1388	2.78
Sport	10000	20	46717	5190	10.38
Taxonomy	10000	31	19416	2157	4.32

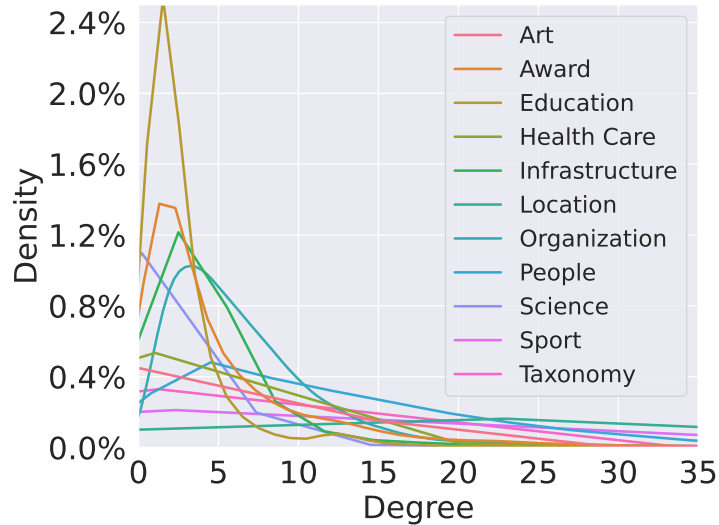


Figure 7: **Statistics of WikiTopics:** We report graph statistics including the number of nodes, number of relations, observed (obv.) triplets, querying (qry.) triplets, and average degree for each graph. We also report (in & out) degree distribution on each graph at the bottom. We omit tail distribution larger than 35 since they are fairly small and almost flat.

1083 against InGram on these benchmarks with results shown in Table 5. We note that, however, due to the different experimental settings (as we discuss next), our results reported in Table 5 are not directly comparable to those reported in Lee et al. (2023) [35], even though they are experimented on essentially the same datasets.

1087 **Difference to the original data split and evaluation in InGram [35]:** Different from Lee et al. (2023) [35], which uses part of the test graph as the validation set to conduct model hyperparameter search, *our experiments consider a harder setting where the relations in test are not observed in the validation data.* Hence, to modify the NL- k , WK- k , and FB- k datasets to our setting, we discard the original validation set and instead split the original training set into a new set of training and validation triplets with a ratio of 9:1. During training, the models perform self-supervised masking over the training set of triplets to create the training-time observable triplets and training-time target triplets. During validation, the entire set of the new training triplets is taken as the validation-time observable triplets, and the new validation triplets are the target triplets to predict. In addition, Lee et al. (2023) [35] evaluate their model’s node prediction performance against *all* nodes in the graph. For efficiency reasons, we evaluate the model performance by sampling without replacement 50 negative nodes for the node prediction task and sampling with replacement 50 negative relation types for the relation prediction task.

1100 Table 5 shows the results, where we can see that ISDEA outperforms InGram on most datasets on the relation prediction task and has smaller standard deviation in general, and DEq-InGram consistently outperforms InGram on all datasets for both relation prediction and node prediction tasks. Importantly, in the dataset FB-100 which follows our doubly inductive link prediction setting with completely new nodes and new relation types in the test with the largest number of training and test relations

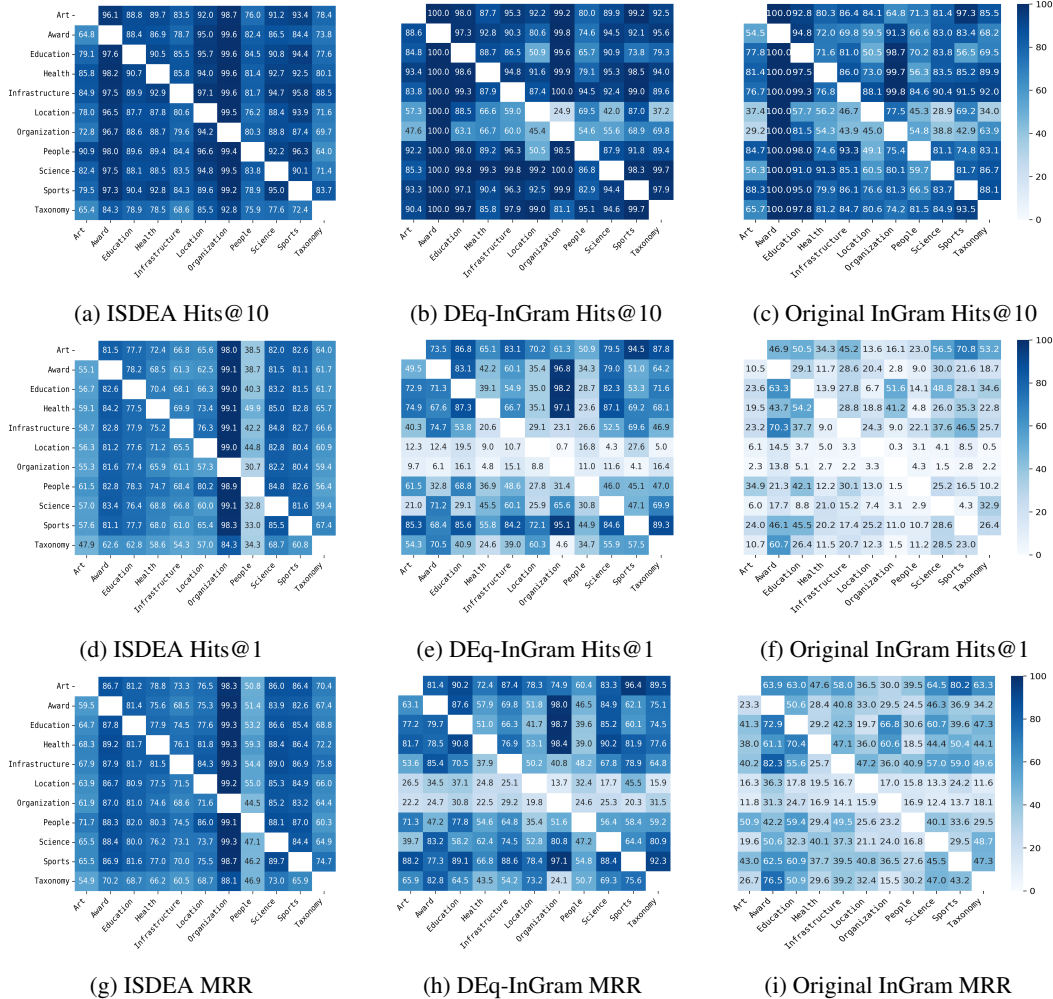


Figure 8: **Relation prediction** (i, j) **performance over WikiTopics** for ISDEA, DEq-InGram, and InGram [35]. Each row within each heatmap corresponds to a training graph, and each column within each heatmap corresponds to a test graph. A darker color means better performance. **Both ISDEA, DEq-InGram perform significantly better than InGram, especially for Hits@1 and MRR, whereas ISDEA exhibits more consistent results across different train-test scenarios than both DEq-InGram and InGram.**

1105 (134 in train and 77 in test) [35], ISDEA achieves significant better results in the relation prediction
 1106 task, showcasing its ability for doubly inductive link prediction.

1107 E.1.5 A Synthetic Case Study for ISDEA

1108 To further understand the expressive power and limitations of our proposed structural double equiv-
 1109 ariant model ISDEA, we create **FD-2** to empirically justify the expressivity of our proposal on tasks
 1110 over both new nodes and new relation types. On FD-2, training has 127 nodes and 2 relations, while
 1111 test has 254 nodes and 4 relations (more nodes and more relations).

1112 FD-2 is constructed by only a single rule, $(E_1, R_1, E_3) \wedge (E_3, R_2, E_2) \Rightarrow (E_1, R_1, E_3)$ where
 1113 E_1, E_2, E_3 and R_1, R_2 are all variables. As illustrated in Figure 10, The training data has only two
 1114 relation types $\{r_1, r_2\}$, while test data has four relation types $\{r_3, r_4, r_5, r_6\}$ which are all different
 1115 from training relations. For all relation types, only r_1, r_3, r_4 can be used for R_1 assignments, and
 1116 only r_2, r_5, r_6 can be use for R_2 assignments. Besides, training and test also have distinct node sets.

1117 Each graph (training or test) is consisted by one or more tree-like structures as left side of Figure 10.
 1118 In each tree-like structure, all solid edges are used as observations, and will form a complete binary

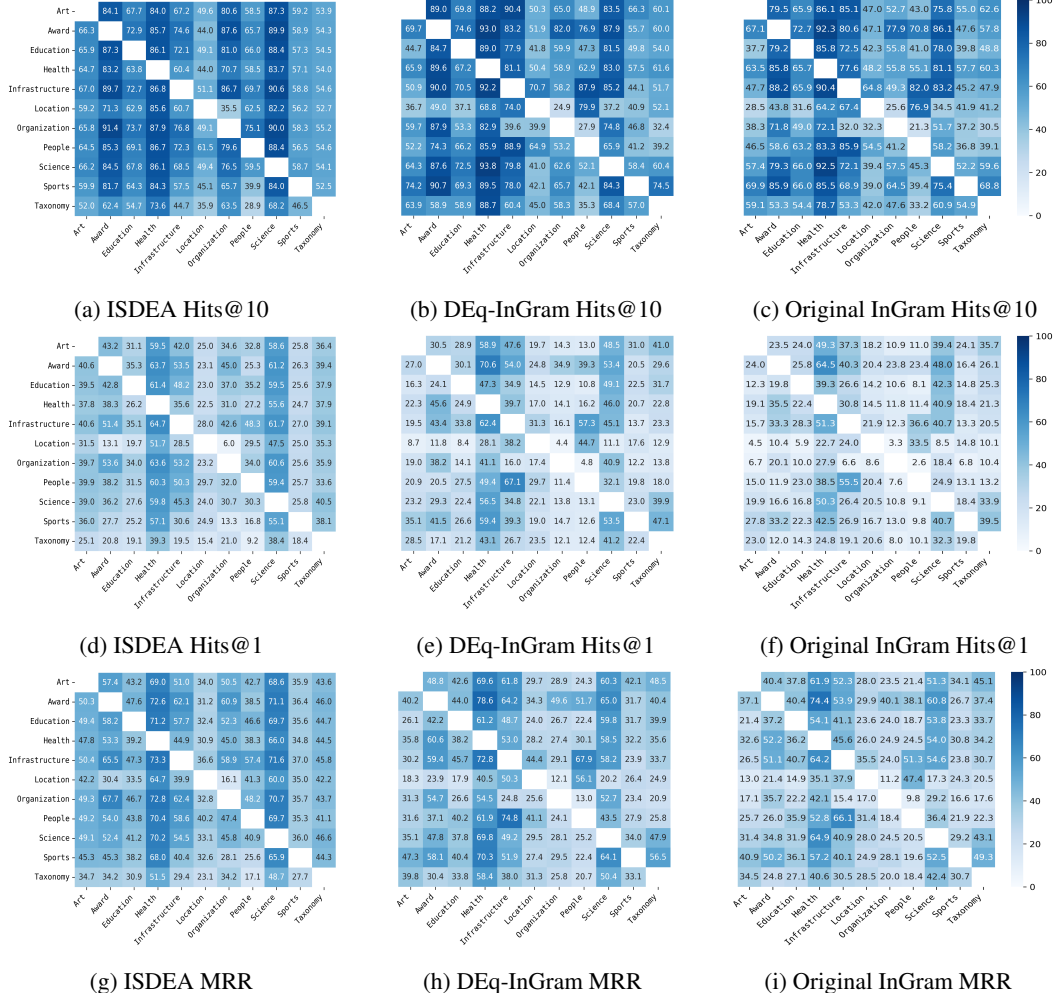


Figure 9: **Node prediction** ($i, k, ?$) **performance over WikiTopics** for ISDEA, DEq-InGram, and InGram [35]. Each row within each heatmap corresponds to a training graph, and each column within each heatmap corresponds to a test graph. A darker color means better performance. **ISDEA, DEq-InGram, and InGram showcase comparable performance in general, and ISDEA exhibits the best performance on Hits@1 in particular.**

1119 tree; while all dashed edges are used as training, validation or test samples which are built by applying
 1120 the only rule over all observed edges. In training, we have only one tree-like structure; while in test,
 1121 we have two disconnected tree-like structures. A more detailed generation algorithm for a graph
 1122 given depths of all tree-like structures is provided in Algorithm 2.

1123 Since the structure of FD-2 does not satisfy the requirement of the spanning tree algorithm used in
 1124 InGram [35], we are not able to apply InGram and DEq-InGram on FD-2. So we provide the results
 1125 on FD-2 in Table 6 with all remaining baselines and ISDEA. We can see that ISDEA clearly perform
 1126 better than other baselines, especially in the relation prediction task, and shows capability to perform
 1127 accurately on the doubly inductive link prediction over both new nodes and new relation types, while
 1128 methods like NBFNet and RMPI are not able to correctly predict this task, even for node prediction.

1129 **E.1.6 Expressivity Limitation Case Study with FD-2 for ISDEA**

1130 We now provide a FD-2 variant where we show that double equivariant representation is not expressive
 1131 enough to solve a specific task. It is a simple 2-depth tree structure as shown in Figure 11. We denote
 1132 node representations given by arbitrary double equivariant representation as $H_{v,r}$ where $v \in [1, 7]$ and

Table 5: **Relation & Node Hits@10 performance on Doubly Inductive Link Prediction over NL- k , WK- k , and FB- k of Lee et al. (2023) [35].** We report standard deviations over 5 runs. A higher value means better doubly inductive link prediction performance. The best values are shown in bold font, while the second-best values are underlined. **ISDEA outperforms InGram on most datasets on the relation prediction task, and DEq-InGram consistently outperforms InGram on all datasets for both relation prediction and node prediction tasks.**

(a) Performance in % on NL- k datasets. Higher \uparrow is better.

Models	Relation prediction ($i, ?, j$)				Node prediction ($i, k, ?$)			
	NL-25	NL-50	NL-75	NL-100	NL-25	NL-50	NL-75	NL-100
InGram	64.54 \pm 16.86	64.54 \pm 12.56	80.16 \pm 04.43	70.84 \pm 08.52	89.95 \pm 02.01	92.74 \pm 00.52	95.40 \pm 01.38	88.20 \pm 01.92
DEq-InGram (Ours)	83.58 \pm 17.57	91.32 \pm 05.60	96.01 \pm 01.23	87.52 \pm 10.39	95.03 \pm 00.32	96.02 \pm 00.34	97.94 \pm 00.34	93.80 \pm 01.38
ISDEA (Ours)	<u>69.49</u> \pm 05.71	<u>76.23</u> \pm 06.92	76.03 \pm 03.31	<u>80.84</u> \pm 07.35	73.74 \pm 03.35	75.76 \pm 03.52	77.27 \pm 03.80	72.81 \pm 04.41

(b) Performance in % on WK- k datasets. Higher \uparrow is better.

Models	Relation prediction ($i, ?, j$)				Node prediction ($i, k, ?$)			
	WK-25	WK-50	WK-75	WK-100	WK-25	WK-50	WK-75	WK-100
InGram	58.76 \pm 13.91	84.01 \pm 03.30	80.19 \pm 04.19	58.20 \pm 11.13	76.99 \pm 07.72	70.93 \pm 02.38	78.85 \pm 04.65	66.29 \pm 03.70
DEq-InGram (Ours)	81.06 \pm 22.31	94.85 \pm 00.85	95.84 \pm 01.54	81.83 \pm 10.10	87.91 \pm 05.68	82.58 \pm 01.70	89.10 \pm 02.15	79.69 \pm 03.07
ISDEA (Ours)	<u>79.49</u> \pm 06.88	81.25 \pm 07.02	<u>84.92</u> \pm 06.86	<u>79.70</u> \pm 07.68	58.28 \pm 23.68	<u>73.24</u> \pm 00.57	76.19 \pm 01.04	<u>71.76</u> \pm 01.85

(c) Performance in % on FB- k datasets. Higher \uparrow is better.

Models	Relation prediction ($i, ?, j$)				Node prediction ($i, k, ?$)			
	FB-25	FB-50	FB-75	FB-100	FB-25	FB-50	FB-75	FB-100
InGram	68.26 \pm 08.27	50.41 \pm 08.79	79.51 \pm 02.69	40.46 \pm 12.21	86.79 \pm 00.70	<u>73.32</u> \pm 06.64	<u>86.57</u> \pm 00.69	71.72 \pm 06.93
DEq-InGram (Ours)	<u>82.89</u> \pm 03.58	<u>76.65</u> \pm 04.05	89.70 \pm 01.14	<u>46.88</u> \pm 15.76	92.39 \pm 00.30	81.08 \pm 06.98	92.14 \pm 00.43	<u>77.54</u> \pm 06.36
ISDEA (Ours)	83.63 \pm 05.66	78.70 \pm 05.90	<u>81.27</u> \pm 07.24	85.41 \pm 04.43	75.93 \pm 00.49	69.90 \pm 00.81	73.45 \pm 01.17	79.70 \pm 00.81

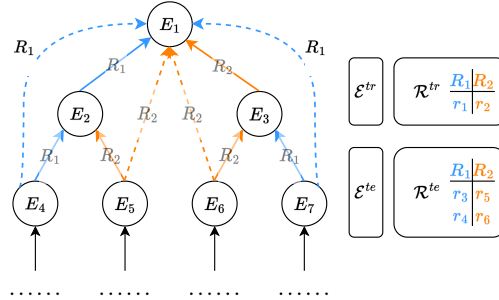


Figure 10: **Synthetic Example of FD-2:** Training and test has their own node and relation type sets: $\mathcal{V}^{(tr)} \cap \mathcal{V}^{(te)} = \emptyset$ and $\mathcal{R}^{(tr)} \cap \mathcal{R}^{(te)} = \emptyset$.

1133 $r \in [1, 4]$. We can easily notice that e_4 and e_7 are symmetric, e_5 and e_6 are symmetric (simply flipping
1134 blue and orange colors), thus we will expect $H_{4,1} = H_{7,2}$, $H_{4,2} = H_{7,1}$, $H_{5,1} = H_{6,2}$, $H_{5,2} = H_{6,1}$.
1135 Since there is no r_3 and r_4 in observation, they are freely exchangeable with each other, thus we will
1136 also expect

$$\begin{aligned}
 H_{1,3} &= H_{1,4}, \\
 H_{4,3} &= H_{4,4} = H_{7,4} = H_{7,3}, \\
 H_{5,3} &= H_{5,4} = H_{6,4} = H_{6,3}.
 \end{aligned}$$

Table 6: **Relation & Node performance on Doubly Inductive Link Prediction over FD2.** We report standard deviations over 5 runs. A higher value means better doubly inductive link prediction performance. The best values are shown in bold font, while the second-best values are underlined. ISDEA consistently achieve better results than the baselines, especially in the Relation prediction task. NA* due to the fact that FD2 does not satisfy the spanning tree algorithm used in InGram [35].

Models	Relation prediction ($i, ?, j$)				Node prediction ($i, k, ?$)			
	MRR	Hits@1	Hits@2	Hits@4	MRR	Hits@1	Hits@2	Hits@4
GAT	7.61±00.71	0.77±00.39	2.78±00.80	5.85±00.95	84.62±02.64	71.61±04.94	93.51±01.03	99.72±00.27
GIN	8.44±00.40	1.29±00.37	3.51±00.58	7.18±01.01	73.99±09.60	65.73±06.58	76.69±12.44	81.45±15.80
GraphConv	7.88±00.45	0.81±00.29	2.62±00.61	6.98±01.09	<u>85.95</u> ±00.77	<u>74.52</u> ±01.81	92.66±01.02	99.84 ±00.15
RMPI	<u>9.09</u> ±03.18	<u>1.94</u> ±01.88	<u>3.95</u> ±04.43	7.10±05.58	21.16±05.85	9.84±05.04	16.74±06.50	27.98±09.96
NBFNet	6.39±02.19	1.50±02.49	1.79±02.39	2.91±02.22	21.95±04.14	14.44±04.34	18.61±04.29	26.47±04.24
InGram	NA*	NA*	NA*	NA*	NA*	NA*	NA*	NA*
DEq-InGram (Ours)	NA*	NA*	NA*	NA*	NA*	NA*	NA*	NA*
ISDEA (Ours)	44.39 ±12.17	32.82 ±12.69	38.71 ±13.60	50.73 ±14.04	90.98 ±03.55	83.59 ±06.22	95.69 ±02.34	<u>99.72</u> ±00.27

Algorithm 2 Synthesis Algorithm for FD-2. This is triplet generation code for a single graph (either training and test). It will provide observation and query triplets. For training, query triplets are further divided into training and validation triplets; For test, query triplets directly become test triplets.

Require: Tree depth $\{D_1, \dots, D_M\}$, Node Labeling “Namesnd”, Relation Type Labeling “Names^{rl}”.

Ensure: Observation triplets \mathcal{S} , Query triplets \mathcal{Q}

```

1:  $\mathcal{S} = \emptyset$ 
2:  $\mathcal{Q} = \emptyset$ 
3:  $n \leftarrow 0$ 
4: for  $m \leftarrow 1, \dots, M$  do
5:   for  $d \leftarrow 1, \dots, D_m$  do
6:     for  $v \leftarrow 2^d - 1, \dots, 2^{d+1} - 2$  do
7:        $u_1 \leftarrow \lceil (v - 2)/2 \rceil$ 
8:        $u_2 \leftarrow \lceil (u_1 - 2)/2 \rceil$ 
9:       if  $v \bmod 2 = 0$  then ▷ For relation type variable  $R_2$ .
10:        if  $u_1 \geq 0$  then
11:           $\mathcal{S}.add((Names^{nd}[n + v], Names^{rl}[2m - 1], Names^{nd}[n + u_1]))$ 
12:        end if
13:        if  $u_2 \geq 0$  then
14:           $\mathcal{Q}.add((Names^{nd}[n + v], Names^{rl}[2m - 1], Names^{nd}[n + u_2]))$ 
15:        end if
16:      else ▷ For relation type variable  $R_1$ .
17:        if  $u_1 \geq 0$  then
18:           $\mathcal{S}.add((Names^{nd}[n + v], Names^{rl}[2m - 2], Names^{nd}[n + u_1]))$ 
19:        end if
20:        if  $u_2 \geq 0$  then
21:           $\mathcal{Q}.add((Names^{nd}[n + v], Names^{rl}[2m - 2], Names^{nd}[n + u_2]))$ 
22:        end if
23:      end if
24:    end for
25:     $n \leftarrow n + 2^d$ 
26:  end for
27: end for

```

1137 After getting all those representations, we can now focus on querying triplet representations (dashed
1138 green and red) by concatenating head and tail node representations w.r.t. relation types:

$$\begin{aligned}
\Gamma_{\text{tri}}((e_1, r_4, e_4), \mathbf{A}) &= H_{1,4} \parallel H_{4,4}, \\
\Gamma_{\text{tri}}((e_1, r_3, e_5), \mathbf{A}) &= H_{1,3} \parallel H_{5,3}, \\
\Gamma_{\text{tri}}((e_1, r_3, e_6), \mathbf{A}) &= H_{1,3} \parallel H_{6,3}, \\
\Gamma_{\text{tri}}((e_1, r_4, e_7), \mathbf{A}) &= H_{1,4} \parallel H_{7,4}.
\end{aligned}$$

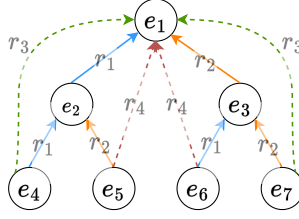


Figure 11: **Expressivity Limitation:** Relation r_1 and r_2 are always observed, while r_3 and r_4 are always querying. r_3 implies that relation types on the path are same, while r_4 implies that relation types on the path are different.

1139 We can notice that

$$\begin{aligned} \underbrace{\Gamma_{\text{tri}}((e_1, r_4, e_4), \mathbf{A})}_{H_{1,4}} \parallel \underbrace{\Gamma_{\text{tri}}((e_1, r_4, e_7), \mathbf{A})}_{H_{4,4}} &= \underbrace{\Gamma_{\text{tri}}((e_1, r_4, e_7), \mathbf{A})}_{H_{1,4}} \parallel \underbrace{\Gamma_{\text{tri}}((e_1, r_3, e_7), \mathbf{A})}_{H_{7,4}} = \underbrace{\Gamma_{\text{tri}}((e_1, r_3, e_7), \mathbf{A})}_{H_{1,3}} \parallel \underbrace{\Gamma_{\text{tri}}((e_1, r_3, e_4), \mathbf{A})}_{H_{7,3}} = \underbrace{\Gamma_{\text{tri}}((e_1, r_3, e_4), \mathbf{A})}_{H_{1,3}} \parallel \underbrace{\Gamma_{\text{tri}}((e_1, r_3, e_5), \mathbf{A})}_{H_{4,3}}, \\ \underbrace{\Gamma_{\text{tri}}((e_1, r_4, e_5), \mathbf{A})}_{H_{1,4}} \parallel \underbrace{\Gamma_{\text{tri}}((e_1, r_4, e_6), \mathbf{A})}_{H_{5,4}} &= \underbrace{\Gamma_{\text{tri}}((e_1, r_4, e_6), \mathbf{A})}_{H_{1,4}} \parallel \underbrace{\Gamma_{\text{tri}}((e_1, r_3, e_6), \mathbf{A})}_{H_{6,4}} = \underbrace{\Gamma_{\text{tri}}((e_1, r_3, e_6), \mathbf{A})}_{H_{1,3}} \parallel \underbrace{\Gamma_{\text{tri}}((e_1, r_3, e_5), \mathbf{A})}_{H_{6,3}} = \underbrace{\Gamma_{\text{tri}}((e_1, r_3, e_5), \mathbf{A})}_{H_{1,3}} \parallel \underbrace{\Gamma_{\text{tri}}((e_1, r_3, e_5), \mathbf{A})}_{H_{5,3}}. \end{aligned}$$

1140 Suppose the score of (e_u, r_c, e_v) utilizing such representation is $s_{u,c,v}$, we will have

$$\begin{aligned} s_{4,4,1} &= s_{7,4,1} = s_{7,3,1} = s_{4,3,1}, \\ s_{5,4,1} &= s_{6,4,1} = s_{6,3,1} = s_{5,3,1}. \end{aligned}$$

1141 If a model can distinguish r_3 and r_4 , it should at least rank node e_7 higher than e_6 given head node e_1
 1142 and relation r_3 since this is a positive triplet in training. Then, we will have $s_{7,3,1} > s_{6,3,1}$, since we
 1143 already knew that $s_{7,3,1} = s_{7,4,1}$, $s_{6,3,1} = s_{6,4,1}$, we will also have $s_{7,4,1} > s_{6,4,1}$. This means that
 1144 we rank node e_7 higher than node e_6 given head node e_1 and relation r_4 , however, this is incorrect
 1145 since (e_7, r_4, e_1) is negative while (e_6, r_4, e_1) is positive. In summary, if we use double equivariant
 1146 representation for triplet scoring in this specific example, there is no way for it to correctly rank r_3
 1147 and r_4 in the same time. This shows that double equivariant representation (even the most expressive)
 1148 can face challenges for doubly inductive link prediction on discrete attributed multigraph.

1149 E.2 Complexity Analysis for ISDEA

1150 For each layer of our method ISDEA, it can be treated as running 2 unattributed GNN $|\mathcal{R}|$ times on the
 1151 attributed multigraph, thus time cost is roughly $2|\mathcal{R}|$ times of adopted GNN. In our experiment, we
 1152 use node representation GNNs (e.g., GIN [73], GAT [65], GraphConv [41]) as our GNN architecture,
 1153 thus the complexity is $\mathcal{O}(|\mathcal{R}||\mathcal{S}|d^3)$ where d is the maximum size of hidden layers, $|\mathcal{R}|$ is number of
 1154 relations in the attributed multigraph, and $|\mathcal{S}|$ is number of fact triplets (number of edges) in attributed
 1155 multigraph.

1156 Besides, for both positive and negative samples (i, k, j) , our method requires the shortest distance
 1157 between any two nodes without considering (i, k, j) . Pay attention that this can not be simply
 1158 achieved from the Dijkstra or Floyd algorithm since the graph changes on computing each node pair,
 1159 indeed computing such distance needs to traverse the enclosed graph [83, 60] between each node pair
 1160 once.

1161 E.3 Ablation study for ISDEA

1162 Since a part of negative samplings is drawn by uniformly corrupting objects (without loss of general-
 1163 ity), it is very likely that corrupted objects are far way from the subject while the true object is close to
 1164 the subject. Then, the distance feature can help predict in such cases. However, the shortest distance
 1165 feature will not provide any additional information if we corrupt the relation type. Under such a
 1166 scenario, shortest distance itself may provide some features to achieve good ranking performance in
 1167 inductive link prediction on attributed multigraph, thus we want to know if shortest distance feature
 1168 augmentation contributes to the performance gain. We perform an ablation study for ISDEA with or
 1169 without distance on doubly inductive link prediction over PediaTypes.

Table 7: **Relation & Node performance on Doubly Inductive Link Prediction over PediaTypes for ISDEA with/without Shortest Distances.** We report standard deviations over 5 runs. A higher value means better doubly inductive link prediction performance. **Even without the shortest distance as an augmented feature, our proposal still achieves comparable results, especially in the relation prediction task.**

(a) Relation prediction ($i, ?, j$) performance in %. Higher \uparrow is better.

Dataset		MRR	Hits@1	Hits@5	Hits@10
EN-FR	ISDEA w/ Distance	70.06±02.01	61.46±00.79	82.11±04.01	84.94±05.00
	ISDEA w/o Distance	68.65±00.41	60.34±00.53	80.17±00.99	82.80±01.73
FR-EN	ISDEA w/ Distance	69.01±00.57	58.18±00.14	83.19±01.73	84.75±02.51
	ISDEA w/o Distance	67.74±01.15	56.35±01.53	83.07±00.75	86.23±00.56
EN-DE	ISDEA w/ Distance	78.38±04.04	68.00±06.41	92.39±00.83	95.26±00.63
	ISDEA w/o Distance	76.52±01.32	67.66±02.37	87.49±00.87	88.47±00.64
DE-EN	ISDEA w/ Distance	88.82±00.28	84.83±00.29	93.59±00.53	94.23±00.71
	ISDEA w/o Distance	88.94±00.92	84.76±00.49	93.98±01.74	94.73±01.98
DB-WD	ISDEA w/ Distance	65.89±04.71	57.51±05.40	75.95±03.89	82.22±02.44
	ISDEA w/o Distance	70.66±07.05	63.36±05.30	79.87±10.19	82.96±11.89
WD-DB	ISDEA w/ Distance	72.57±00.73	62.72±01.24	86.10±01.26	88.87±02.94
	ISDEA w/o Distance	67.98±02.14	60.83±01.55	76.65±03.14	77.90±03.09
DB-YG	ISDEA w/ Distance	75.88±01.58	69.12±02.40	85.80±01.23	91.42±01.79
	ISDEA w/o Distance	75.42±00.35	69.17±01.13	84.86±01.58	88.78±02.36
YG-DB	ISDEA w/ Distance	74.04±00.47	66.68±00.81	83.36±01.55	85.34±01.49
	ISDEA w/o Distance	74.22±01.56	66.97±01.63	83.62±01.85	85.73±02.66

(b) Node prediction ($i, k, ?$) performance in %. Higher \uparrow is better.

Dataset		MRR	Hits@1	Hits@5	Hits@10
EN-FR	ISDEA w/ Distance	53.92±00.26	43.03±00.25	64.45±00.24	76.28±00.50
	ISDEA w/o Distance	45.12±00.41	34.04±00.36	56.61±00.48	63.46±00.76
FR-EN	ISDEA w/ Distance	57.68±00.68	47.38±00.28	67.24±01.32	77.51±01.46
	ISDEA w/o Distance	42.52±00.91	30.41±01.17	54.94±00.22	65.29±00.20
EN-DE	ISDEA w/ Distance	50.30±02.08	35.41±02.25	68.80±01.90	82.24±00.94
	ISDEA w/o Distance	45.16±00.76	30.26±00.76	62.59±00.57	76.98±00.63
DE-EN	ISDEA w/ Distance	51.33±00.40	37.12±00.31	68.20±00.53	81.80±00.68
	ISDEA w/o Distance	43.67±00.32	28.97±00.25	60.36±00.54	74.95±00.51
DB-WD	ISDEA w/ Distance	45.75±00.66	35.59±00.73	54.83±00.90	66.69±01.01
	ISDEA w/o Distance	40.26±03.77	30.59±03.89	48.15±03.68	59.43±03.76
WD-DB	ISDEA w/ Distance	51.64±00.60	40.56±01.72	62.60±02.55	75.19±03.12
	ISDEA w/o Distance	45.94±00.14	35.17±00.30	56.89±00.33	66.46±00.55
DB-YG	ISDEA w/ Distance	41.72±01.64	27.70±01.95	55.21±01.07	72.87±01.03
	ISDEA w/o Distance	32.71±00.60	17.69±00.39	47.82±00.60	66.92±01.90
YG-DB	ISDEA w/ Distance	48.21±01.06	35.29±01.67	61.87±01.30	76.41±01.52
	ISDEA w/o Distance	37.52±00.79	23.10±00.76	53.34±00.88	68.43±01.62

1170 As shown in Table 7, even if the shortest distance is excluded from our model, our model still
 1171 performs quite well and is better than most other baselines in the doubly inductive link prediction on
 1172 PediaTypes. Especially, as we anticipate, the distance feature is more helpful in the node prediction
 1173 task than the relation prediction task. Thus, we can say that double equivariant node representation
 1174 itself is enough to provide good performance on doubly inductive link prediction.

1175 E.4 Limitations and Impacts for ISDEA

1176 ISDEA excels both in synthetic and real-world benchmarks. However, the simplification from
 1177 pairwise to node embeddings in ISDEA limits its expressivity. In Appendix E.1.5, we give a synthetic
 1178 counterexample how this could be an issue in some attributed multigraphs. Moreover, ISDEA has the
 1179 same pre-processing scalability as GraIL. We also do not envision a direct negative social impact of
 1180 our work.

1181 **F Future Work**

1182 As addressed in the main paper, our implemented architecture ISDEA has a few limitations, which
1183 could be addressed in future work. First, ISDEA has high pre-processing cost. This high time cost
1184 is introduced by using shortest distances whose computation is of the same complexity as enclosed
1185 subgraph. However, our ablation studies show that shortest distances is not a dominant factor in
1186 our model for real-world tasks, thus it is possible that shortest distances can be replaced by other
1187 heuristics that can be efficiently extracted.

1188 Second, our specific implementation ISDEA happens to have high training and inference costs, since
1189 it relies on repeating GNNs for each relation. Thus, complexity ISDEA of scales linearly w.r.t. number
1190 of relations, which is often a large number in real-world knowledge base, e.g., Wikipedia. However,
1191 fully equivariance over all relations can be too strong, and we may only want partial equivariance
1192 which may reduce the cost.

1193 Third, ISDEA has expressivity limitation. This limitation is related to former two cost issues since it
1194 is caused by compromising most-expressive pairwise representation to node-wise representation due
1195 to time cost. Thus if we can reduce the cost, we may be able to use more expressive graph encoder.

1196 Finally, although we show ISDEA representations can capture UQER Horn clauses, there is no
1197 algorithm to create UQER Horn clauses from ISDEA representations. This topic is known as
1198 *explainability* which is important in graph machine learning community. We leave such an algorithm
1199 as another future work other than optimization.